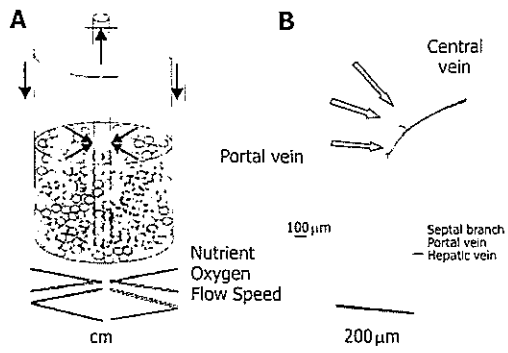

Figure 11 RFB and intact organ. A: In the RFB system, culture medium flows from outside the column toward the center of the reactor. Medium flows faster at the center than at the periphery. Biases in distribution of oxygen and nutrition at inflow and outflow are minimized. B: In the hepatic lobe, blood flows from the portal vein to central vein. The RFB system is similar to the organization of the hepatic primary lobe[31]. Figure 11B is reproduced from Figure 9 in reference 31.

tion in OTC-deficient mice could be detected under the same condition[27]. Glutamic acid, glutamine and alanine were also increased in supernatant co-cultured in the RFB, indicating that amino acid metabolism becomes active.

It was reported that three-dimensional spherical culture induces albumin synthesis, a particularly important hepatocytic function[28, 29]. However, in the present study, mRNA expression of albumin was decreased under coculture conditions in the RFB. Nuclear transcriptional factors HNF-4 and HNF-1, which regulate albumin synthesis, were decreased under coculture conditions in the RFB. Albumin in supernatant was also decreased during culture (data not shown). The results suggest that the culture environment (cell-to-cell communication, cell polarity, shear stress, and other factors) can control manifestations of intracellular nuclear transcription factors and therefore dramatically influence albumin production by liver cells. Immortalized cells can be used for artificial liver. The reason is that it can supply cells in large quantities and quickly. But immortalized cells may change the characteristics of its original cells. In this study, albumin synthesis was decreased. It was not useful for artificial liver. In future study, we have to try other cell sources (ES cell, oval cell, and other immortalized cell lines).

Finally, several points should be noted concerning our culture system. First, controlling the mixture ratio of the three cell types used is very difficult since each type possesses its own potential for active growth. Thus, growth rates vary between cell types and are difficult to control. For examples, A7 cells grew less rapidly and tended to be less than the other two cell types in the coculture system. Second, the hepatic lobule spans about 140 μm *in vivo*, extending from the portal to the central area, toward which portal blood flows in a radial manner. According to Matsumoto *et al*[30], the liver is an organ composed of numerous groups of microscopic three-dimensional units (minimal radial-flow bioreactors) extending from the inflow side (composed of combinations of parabola-shaped inflow fronts) to the central vein[31]. According to this model, the liver microcirculation as observed *in vivo* could not be reproduced faithfully with a radial-flow bioreactor, since the distance between inflow and outflow sides in the bioreactor is about 1.5 cm (Figure 11). Third, bile canaliculus-like structures are formed between hepatocytes. Since we did not use the bile duct cells in this study, whether different cell types can reconstruct bile ducts remains to be elucidated[32]. Finally, although several questions remain, the results of the present study suggest that liver reconstruction is possible *in vitro*. Such organ reconstruction technology is expected to contribute greatly to the development of sophisticated artificial livers and other organs for transplantation. Our culture system may be a very important tool to maintain liver organ.

ACKNOWLEDGMENTS

The authors thank Mr. Hideki Saito, Mrs. Emi Kikuchi, and Mrs. Hisako Arai of the DNA Medical Institute at The Jikei University School of Medicine for technical assistance with electron microscopy. The authors also thank the members of the Australian Key Center for Microscopy and Microanalysis of The University of Sydney for their excellent administrative, technical, and practical support.

REFERENCES

1 **Gordon GJ**, Butz GM, Grisham JW, Coleman WB. Isolation, short-term culture, and transplantation of small hepatocyte-like progenitor cells from retrorsine-exposed rats. *Transplantation* 2002; 73: 1236-1243
2 **Kanda T**, Watanabe S, Yoshiike K. Immortalization of primary rat cells by human papillomavirus type 16 subgenomic DNA fragments controlled by the SV40 promoter. *Virology* 1988; 165: 321-325
3 **Nishida K**, Yamato M, Hayashida Y, Watanabe K, Yamamoto K, Adachi E, Nagai S, Kikuchi A, Maeda N, Watanabe H, Okano T, Tano Y. Corneal reconstruction with tissue-engineered cell sheets composed of autologous oral mucosal epithelium. *N Engl J Med* 2004; 351: 1187-1196
4 **Nishida K**, Yamamoto M, Hayashida Y. Corneal reconstruction using tissue-engineered cell sheets comprising autologous oral mucosal epithelium. *N Engl J Med* 2004; 351: 1187-1196
5 **Tabata Y**. Tissue regeneration based on growth factor release. *Tissue Eng* 2003; 9 **Suppl** 1: S5-S15
6 **Sussman NL**, Chong MG, Koussayer T, He DE, Shang TA, Whisennand HH, Kelly JH. Reversal of fulminant hepatic failure using an extracorporeal liver assist device. *Hepatology* 1992; 16: 60-65
7 **Sussman NL**, Kelly JH. Improved liver function following treatment with an extracorporeal liver assist device. *Artif Organs* 1993; 17: 27-30
8 **Matsuura T**, Kawada M, Hasumura S, Nagamori S, Obata T, Yamaguchi M, Hataba Y, Tanaka H, Shimizu H, Unemura Y, Nonaka K, Iwaki T, Kojima S, Aizaki H, Mizutani S, Ikenaga H. High density culture of immortalized liver endothelial cells in the radial-flow bioreactor in the development of an artificial liver. *Int J Artif Organs* 1998; 21: 229-234
9 **Matsuura T**, Kawada M, Sujino H, Hasumura S, Nagamori S, Shimizu H. Vitamin A metabolism of immortalized hepatic stellate cell in the bioreactor. In: Wisse E, Knook D L, De Zanger R, Arthur M J P, eds. Cells of the Hepatic Sinusoid 7. Leiden: *Kupffer Cell Foundation*, 1999: 88-89
10 Jat PS, Noble MD, Ataliotis P, Tanaka Y, Yannoutsos N, Larsen L, Kioussis D. Direct derivation of conditionally immortal cell lines from an H-2Kb-tsA58 transgenic mouse. *Proc Natl Acad Sci USA* 1991; 88: 5096-5100
11 Wisse E. An electron microscopic study of the fenestrated endothelial lining of rat liver sinusoids. *J Ultrastruct Res* 1970; 31:

125-150
12 **Braet F.** How molecular microscopy revealed new insights into the dynamics of hepatic endothelial fenestrae in the past decade. *Liver Int* 2004; 24: 532-539
13 **Fraser R,** Dobbs BR, Rogers GW. Lipoproteins and the liver sieve: the role of the fenestrated sinusoidal endothelium in lipoprotein metabolism, atherosclerosis, and cirrhosis. *Hepatology* 1995; 21: 863-874
14 **Braet F,** Spector I, De Zanger R, Wisse E. A novel structure involved in the formation of liver endothelial cell fenestrae revealed by using the actin inhibitor misakinolide. *Proc Natl Acad Sci USA* 1998; 95: 13635-13640
15 **Braet F,** Spector I, Shochet N, Crews P, Higa T, Menu E, de Zanger R, Wisse E. The new anti-actin agent dihydrohalichondramide reveals fenestrae-forming centers in hepatic endothelial cells. *BMC Cell Biol* 2002; 3: 7
16 **Oda M,** Tsukada N, Komatsu H, Kaneko K, Nakamura M, Tsuchiya M: Electron microscopic localizations of actin, calmodulin and calcium in the hepatic sinusoidal endothelium in the rat. In: Kim A, Knook DL, Wisse E des. Cells of the Hepatic Sinusoid 1. Rijswijk, *Kupffer Cell Foundation* 1986, 511-512
17 **Gatmaitan Z,** Varticovski L, Ling L, Mikkelsen R, Steffan AM, Arias IM. Studies on fenestral contraction in rat liver endothelial cells in culture. *Am J Pathol* 1996; 148: 2027-2041
18 **Kawada M,** Nagamori S, Aizaki H, Fukaya K, Niiya M, Matsuura T, Sujino H, Hasumura S, Yashida H, Mizutani S, Ikenaga H. Massive culture of human liver cancer cells in a newly developed radial flow bioreactor system: ultrafine structure of functionally enhanced hepatocarcinoma cell lines. *In Vitro Cell Dev Biol Anim* 1998; 34: 109-115
19 **Aizaki H,** Nagamori S, Matsuda M, Kawakami H, Hashimoto O, Ishiko H, Kawada M, Matsuura T, Hasumura S, Matsuura Y, Suzuki T, Miyamura T. Production and release of infectious hepatitis C virus from human liver cell cultures in the three-dimensional radial-flow bioreactor. *Virology* 2003; 314: 16-25
20 **Braet F,** de Zanger R, Seynaeve C, Baekeland M, Wisse E. A comparative atomic force microscopy study on living skin fibroblasts and liver endothelial cells. *J Electron Microsc (Tokyo)* 2001; 50: 283-290
21 **Feng D,** Nagy JA, Hipp J, Dvorak HF, Dvorak AM. Vesiculovacuolar organelles and the regulation of venule permeability to macromolecules by vascular permeability factor, histamine, and serotonin. *J Exp Med* 1996; 183: 1981-1986
22 **Feng D,** Nagy JA, Pyne K, Hammel I, Dvorak HF, Dvorak AM. Pathways of macromolecular extravasation across microvascular endothelium in response to VPF/VEGF and other vasoactive mediators. *Microcirculation* 1999; 6: 23-44
23 **Yokomori H,** Oda M, Yoshimura K, Nagai T, Ogi M, Nomura M, Ishii H. Vascular endothelial growth factor increases fenestral permeability in hepatic sinusoidal endothelial cells. *Liver Int* 2003; 23: 467-475
24 **Oda M,** Yokomori H, Han J Y, Kamegaya Y, Ogi M, Nakamura M. Hepatic sinusoidal endothelial fenestrae are a stationary type of fused and interconnected caveolae. In: Wisse E, Knook D L, De Zanger R, Arthur M J P, eds. Cells of the Hepatic Sinusoid 8. Leiden: *Kupffer Cell Foundation*, 2001: 94-98
25 **Nagamori S,** Hasumura S, Matsuura T, Aizaki H, Kawada M. Developments in bioartificial liver research: concepts, performance, and applications. *J Gastroenterol* 2000; 35: 493-503
26 **Iwahori T,** Matsuura T, Maehashi H, Sugo K, Saito M, Hosokawa M, Chiba K, Masaki T, Aizaki H, Ohkawa K, Suzuki T. CYP3A4 inducible model for in vitro analysis of human drug metabolism using a bioartificial liver. *Hepatology* 2003; 37: 665-673
27 **Li MX,** Nakajima T, Fukushige T, Kobayashi K, Seiler N, Saheki T. Aberrations of ammonia metabolism in ornithine carbamoyltransferase-deficient spf-ash mice and their prevention by treatment with urea cycle intermediate amino acids and an ornithine aminotransferase inactivator. *Biochim Biophys Acta* 1999; 1455: 1-11
28 **Glicklis R,** Merchuk JC, Cohen S. Modeling mass transfer in hepatocyte spheroids via cell viability, spheroid size, and hepatocellular functions. *Biotechnol Bioeng* 2004; 86: 672-680
29 **Ma M,** Xu J, Purcell WM. Biochemical and functional changes of rat liver spheroids during spheroid formation and maintenance in culture: I. morphological maturation and kinetic changes of energy metabolism, albumin synthesis, and activities of some enzymes. *J Cell Biochem* 2003; 90: 1166-1175
30 **MacSween R.** N. M. Pathology of the Liver, 4th ed. In: Developmental anatomy and normal structure, *Churchill Livingstone*, 2002: 16-22
31 **Matsumoto T,** Komori R, Magara T, Ui T, Kawakami M, Hano H. A study on the normal structure of the human liver, with special reference to its angioarchitecture. *Jikei Med J* 1979; 26: 1-40
32 **Ishida Y,** Smith S, Wallace L, Sadamoto T, Okamoto M, Auth M, Strazzabosco M, Fabris L, Medina J, Prieto J, Strain A, Neuberger J, Joplin R. Ductular morphogenesis and functional polarization of normal human biliary epithelial cells in three-dimensional culture. *J Hepatol* 2001; 35: 2-9

S- Editor Wang J L- Editor Wang XL E- Editor Liu WF

ELSEVIER

Journal of Hepatology 45 (2006) 190–196

Journal of Hepatology

www.elsevier.com/locate/jhep

Enhanced ability of peripheral invariant natural killer T cells to produce IL-13 in chronic hepatitis C virus infection

Michiyo Inoue[1], Tatsuya Kanto[1], Hideki Miyatake[2], Ichiyo Itose[2], Masanori Miyazaki[2], Takayuki Yakushijin[2], Mitsuru Sakakibara[2], Noriyoshi Kuzushita[2], Naoki Hiramatsu[2], Tetsuo Takehara[2], Akinori Kasahara[3], Norio Hayashi[2,*]

[1]*Department of Dendritic Cell Biology and Clinical Application, Osaka University Graduate School of Medicine, Osaka, Japan*
[2]*Department of Gastroenterology and Hepatology, Osaka University Graduate School of Medicine, 2-2 Yamada-oka, Suita, Osaka 565-0871, Japan*
[3]*Department of General Medicine, Osaka University Graduate School of Medicine, Osaka, Japan*

***Background/Aims*: Human invariant natural killer T (iNKT) cells express a TCR Vα24-JαQ paired with Vβ11 and are activated by a surrogate ligand, α-galactosylceramide (αGalCer). The iNKT cells are involved in the regulation of antiviral immune responses; however, little is known about their roles in hepatitis C virus (HCV) infection.**

***Methods*: We compared the frequency of peripheral iNKT cells and their cytokine producing capacity reactive to αGalCer between chronically HCV-infected patients and healthy subjects. Cytokine production of freshly isolated iNKT cells were analyzed by ELISPOT. Activated iNKT cells were obtained by culture with αGalCer-loaded dendritic cells (DCs) and re-stimulated with them for the measurement of cytokine production.**

***Results*: The frequencies of iNKT cells were not different between HCV-infected patients and healthy subjects. The number of fresh IFN-γ-producing iNKT cells reactive to αGalCer was not different between the patients and controls, whereas fresh iNKT cells produced negligible amounts of Th2 cytokines regardless of HCV infection. In response to αGalCer, expanded iNKT cells from the patients secreted IFN-γ comparable in amount to controls, whereas they released significantly more IL-13 than cells from controls.**

***Conclusions*: Activated iNKT cells from HCV-infected patients gain more ability to secrete IL-13 than those from healthy subjects.**

Keywords: Hepatitis C virus; Natural killer T cell; Th1; Th2; α-Galactosylceramide

1. Introduction

Hepatitis C virus (HCV) frequently gives rise to chronic liver disease, which varies from asymptomatic HCV carriers to liver cirrhosis and hepatocellular carcinoma (HCC) [1]. Cumulative reports have demonstrated that innate as well as adaptive immune responses are involved in the pathogenesis of HCV-induced liver injury and the development of liver disease [2,3].

Natural killer T (NKT) cells are a unique lymphocyte subset co-expressing T-cell receptor (TCR) and NK cell markers [4]. The NKT cell population is highly heterogeneous; invariant NKT (iNKT) cells express an invariant TCR, composed of Vα24-JαQ preferentially paired with Vβ11 in humans [4,5], whereas non-invariant NKT cells express diverse TCR. Invariant NKT cells recognize glycolipid antigens presented on the non-polymorphic MHC class I-like molecule CD1d [6,7], which is expressed by antigen presenting cells, such as dendritic cells (DCs). Although endogenous ligands of iNKT cells are little known, α-galactosylceramide (αGalCer) has

Received 28 December 2005; accepted 17 January 2006; available online 28 February 2006

* Corresponding author. Tel.: +81 6 6879 3621; fax: +81 6 6879 3629.
E-mail address: hayashin@gh.med.osaka-u.ac.jp (N. Hayashi).

0168-8278/$32.00
doi:10.1016/j.jhep.2006.01.034

been used as a surrogate for natural ligands. It has been demonstrated that phenotypic as well as functional subsets exist for iNKT cells, which are CD4+, CD4–CD8– double-negative (DN) and CD8+ ones. The CD4+ and DN iNKT cells produce both Th1 (interferon (IFN)-γ) and Th2 cytokines (interleukin (IL)-4, IL-5, IL-13). The CD4+ iNKT cells secrete more Th2 cytokines than DN, while CD8+ subsets predominantly secrete Th1 cytokines [8].

Although iNKT cells comprise a small portion of hemotopoietic cells, they regulate various immune responses by secreting Th1 as well as Th2 cytokines in clinical settings, such as autoimmune disease, viral infection or cancer [9–13]. For chronic HCV infection, there have been some controversial reports about the frequency of peripheral iNKT cells [14–16], however, their functional roles in HCV-infected patients are largely unknown. We compared the frequency and the cytokine producing capacity of iNKT cells in fresh peripheral blood between chronic hepatitis C patients and healthy individuals. Furthermore, to analyze the functions of activated iNKT cells, we expanded iNKT cells by stimulation with αGalCer-loaded DCs. Of note, in response to αGalCer-pulsed DCs, the activated iNKT cells obtained from chronic hepatitis C patients secreted a significantly larger amount of IL-13 and tend to produce more IL-4 and IL-5 than those from healthy subjects, indicating that peripheral iNKT cells may be involved in the pathogenesis of chronic hepatitis C.

2. Materials and methods

2.1. Subjects

After informed consent had been obtained, 19 patients who were positive for both anti-HCV Ab and serum HCVRNA were enrolled in this study (chronic hepatitis [CH] group). All patients were negative for hepatitis B virus (HBV) and human immunodeficiency virus (HIV) and had no apparent history of other types of liver diseases. The HCV serotype of all patients was type 1. None of them had been treated with anti-viral agents, such as IFN-α or ribavirin. As controls, 18 age-matched healthy subjects (HS group) who were negative for HCV, HBV and HIV were examined. The clinical backgrounds of the patients and healthy subjects are shown in Table 1.

Table 1
Clinical backgrounds of healthy subjects and chronic hepatitis C patients

	Healthy subjects	Chronic hepatitis C patients
N (M/F)	18 (13/5)	19 (11/8)
Age[a]	38 ± 9	48 ± 14
Serum ALT (IU/L)[b]	ND	58 (23–238)
HCVRNA (Mequiv./ml)[b]	ND	2.5 (0.5–15.0)

[a] Values are expressed as mean ± SD.

[b] Median with range in parentheses. ALT, alanine aminotransferase; Mequiv./ml, million genome equivalents per milliliter; ND, not determined.

2.2. Reagents

Recombinant human granulocyte-macrophage colony-stimulating factor (GM-CSF) and IL-4 were purchased from Peprotech (London, UK). Recombinant human IL-2 was from Genzyme (Minneapolis, MN). αGalCer was provided by Kirin Brewery (Gumma, Japan).

2.3. Generation of monocyte-derived DCs

To stimulate iNKT cells, monocyte-derived DCs (Mo-DCs) were generated from CD14+ cells. CD14+ cells were separated from peripheral blood mononuclear cells (PBMCs) with anti-CD14 microbeads (Miltenyi Biotec, Bergisch Gladbach, Germany). They were cultured at 5×10^5/well in the DC culture media (DCM) (IMDM supplemented with 10% FCS, 100 U/ml penicillin, 100 μg/ml streptomycin, 10 mM HEPES buffer, 1 mM non-essential amino acid and 2 mM L-glutamine) containing 100 ng/ml GM-CSF and 20 ng/ml IL-4 for 7 days. For maturation of the DCs, they were given 50 μg/ml *Staphylococcus aureus Cowan I* (SAC) on day 6 of the culture. αGalCer (100 ng/ml) was pulsed to the DCs on the same day.

2.4. Frequency and phenotype analyses of iNKT cells in peripheral blood

PBMCs were isolated from the venous blood of HCV-positive patients or healthy subjects by Ficoll–Hypaque density-gradient centrifugation. For staining, PBMCs were incubated with fluorescence-labeled Abs for 30 min at 4 °C in PBS supplemented with 1% BSA and 0.1% NaN_3. The stained cells were analyzed using FACS Calibur and Cell Quest software (Becton Dickinson, San Jose, CA). For the measurement of iNKT cell subsets, the cells were stained with a combination of anti-Vα24, anti-Vβ11 and anti-CD4 mAbs (Immunotech, Marseilles, France). The frequencies of total (Vα24+, Vβ11+), CD4-positive (Vα24+, Vβ11+, CD4+) and CD4-negative (Vα24+, Vβ11+, CD4–) iNKT cells were determined. To examine iNKT cell phenotypes, they were further stained with mAbs against CCR7, CXCR3 (R&D Systems, Minneapolis, MN), CCR4, CD62L (BD Pharmingen, San Jose, CA) and analyzed by FACS Calibur.

2.5. Cytokine analysis of peripheral iNKT cells in response to αGalCer

For enumeration of the peripheral IFN-γ-producing cells in response to αGalCer, we used enzyme-linked immunospot (ELISPOT) assay. MultiScreen® ELISPOT plates (Millipore, Bedford, MA) were coated with 10 μg/ml mouse anti-human IFN-γ mAb (1-D1K, Mabtech, Sweden). Monocyte-depleted PBMCs were cultured at 5×10^5/well with 5×10^4/well autologous Mo-DCs pulsed with or without αGalCer for 24 h on Ab-coated plates. PBMCs pulsed with PHA (1 μg/ml) were used as positive controls. After 24 h, the culture supernatants were collected for ELISA. Subsequently, the plates were washed and then incubated with biotin-labeled anti-human IFN-γ mAb (7-B6-1, Mabtech). After addition of streptavidin-HRP to the plates, spots were developed using 3-amino-9-ethylcarbazole (Sigma–Aldrich, St Louis, MO). Spots corresponding to IFN-γ-secreting cells were identified by microscopy and counted by two independent observers. The number of αGalCer-reactive IFN-γ-producing cells was determined by subtracting the number of spot-forming cells with αGalCer-unpulsed Mo-DCs from those with αGalCer-pulsed ones. To confirm that cytokines were released from iNKT cells, we also examined Vα24-depleted and/or Vβ11-depleted cells stimulated with αGalCer-pulsed Mo-DCs. Vα24-positive or Vβ11-positive cells was depleted with mouse anti-human Vα24 or Vβ11 mAbs (Immunotech) and subsequently anti-mouse IgG microbeads (Miltenyi Biotec). The Vα24-positive

or Vβ11-positive cells remaining in the treated samples were less than 5% as assessed by FACS (data not shown).

2.6. Expansion of iNKT cells from peripheral blood and analyses of cytokine production from them

To investigate the ability of activated iNKT cell subsets to proliferate and produce cytokines in response to αGalCer, we expanded them according to a method described previously [17] with some modifications. Monocyte-depleted PBMCs were cultured at 3×10^6/well with 3×10^5/well αGalCer-loaded autologous mature Mo-DCs for 2 weeks in DCM containing 5 ng/ml IL-2. For stimulation of the cells, 2.5 ng/ml IL-2 was added to the culture every 3 days. Subsequently, Vα24+ cells were magnetically separated and cultured in DCM for additional 3 weeks, which were fed with 2.5 ng/ml IL-2 every 3 days. Finally, the cells were stained with fluorescence-labeled mAbs against Vα24, Vβ11 and CD4. At this point, the rates of increase of total, CD4-positive and CD4-negative iNKT cells were calculated from the absolute numbers of relevant cells before and after the culture. Vα24+Vβ11+CD4+ cells and Vα24+Vβ11+CD4− cells were sorted by FACS Vantage (Becton Dickinson). The sorted cells whose purity was more than 85%, were used for cytokine producing analysis. Sorted iNKT cells were cultured at 1×10^5/well with 1×10^4/well αGalCer-pulsed or unpulsed allogenic mature Mo-DCs for 24 h. Mo-DCs as stimulators were obtained from the same donor. The supernatants of the culture were collected for cytokine ELISA.

2.7. ELISA

IFN-γ, IL-4, IL-5 and IL-13 concentrations of the supernatants were measured by ELISA. The paired Abs and standards were purchased from Endogen (Woburn, MA). The ranges of the assay were 0–1000 pg/ml for IFN-γ and IL-13, and 0–500 pg/ml for IL-4 and IL-5, respectively.

2.8. Statistical analysis

Statistical analysis was performed using the Mann–Whitney *U*-test (StatView, SAS Institute, Cary, NC). A *P*-value of less than 0.05 was taken as statistically significant.

3. Results

3.1. Frequencies of peripheral iNKT cell subsets in chronic hepatitis C patients are comparable to those in healthy subjects

Human CD1d-restricted iNKT cells express a conserved canonical TCR α-chain (Vα24-JαQ) paired with TCR β-chain (Vβ11). Thus, we examined the frequencies of peripheral Vα24+Vβ11+ cells as iNKT cells in the CH and HS groups. Although the frequencies of these cells showed a wide range of distribution in both groups (HS = 0.01–0.61%, CH = 0.01–0.43%), no difference was observed in total iNKT cells and their CD4+ and CD4− subsets between the CH and the HS group (Fig. 1). In both CH and HS groups, there was no correlation between any of the iNKT frequencies and age, serum HCVRNA titers or alanine aminotransferese (ALT) levels (data not shown).

3.2. Peripheral iNKT cell subsets in chronic hepatitis C patients express higher levels of CXCR3 than in healthy subjects

Next, we examined the expressions of some chemokine receptors and homing receptor on peripheral iNKT cell subsets. The expression of CXCR3 on both subsets in the CH group was higher than that in the HS group (Fig. 2), whereas those of the others (CCR4, CCR7 or CD62L) were not different between the groups (Fig. 2).

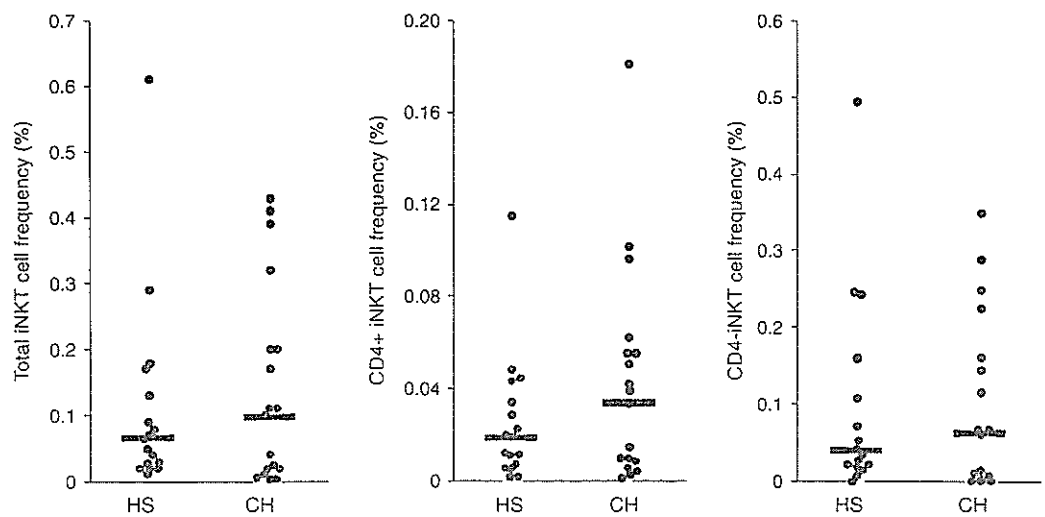

Fig. 1. Frequency of peripheral iNKT cell subsets in healthy subjects and chronic hepatitis C patients. The frequencies of total, CD4-positive and CD4-negative iNKT cells in PBMCs were determined by flow cytometry as described in Section 2. HS, healthy subjects; CH, chronic hepatitis C patients. Horizontal bars represent the median.

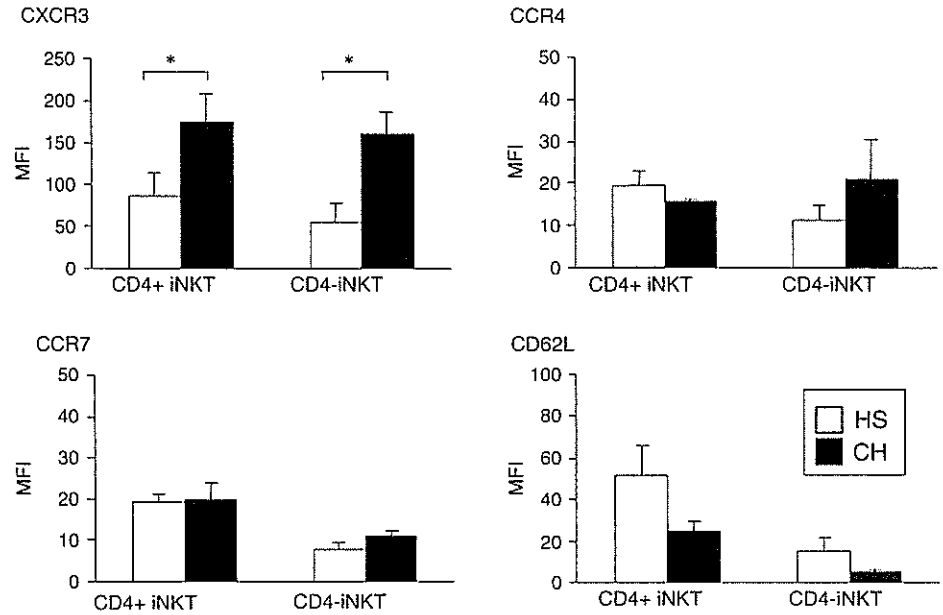

Fig. 2. Expressions of chemokine receptors and homing receptor on peripheral iNKT cell subsets in healthy subjects and chronic hepatitis C patients. The *y*-axis indicates the mean fluorescence intensity (MFI) of the expression of each receptor as determined by flow cytometry. The bars represent mean + SE of six different subjects. The white column represents the healthy subject group and the black one represents the chronic hepatitis C group. HS, CH, as in Fig. 1. *$P < 0.05$ by Mann–Whitney *U*-test.

3.3. The IFN-γ-producing capacity of peripheral iNKT cells in response to αGalCer in chronic hepatitis C patients is comparable with those in healthy subjects

With respect to the αGalCer-responsive IFN-γ-producing cells in PBMCs, the ELISPOT assay in this study detected as few as 10 spots/5×10^5 cells. When samples depleted of Vα24+ or Vβ11+ cells were used, the numbers of spots were significantly reduced, indicating that Vα24+ or Vβ11+ cells mainly released IFN-γ in response to αGalCer (data not shown). The numbers of IFN-γ-producing cells reactive to αGalCer in the peripheral blood were not different between the CH and the HS groups (Fig. 3). No correlation was observed between IFN-γ-producing cell number and serum HCVRNA titers or ALT levels. The levels of IL-4 and IL-13 in the supernatants were below the thresholds of ELISA (data not shown).

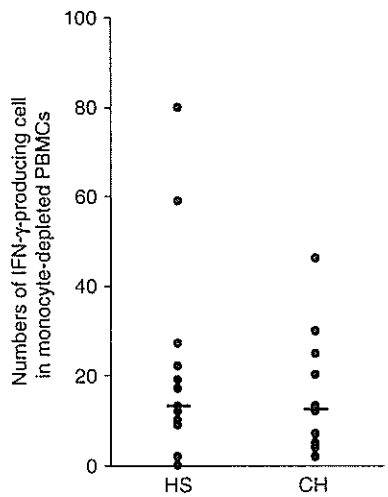

Fig. 3. Numbers of IFN-γ-producing cells in fresh PBMC stimulated with αGalCer-pulsed Mo-DCs. After monocyte-depleted PBMCs were co-cultured with αGalCer-pulsed autologous Mo-DCs for 24 h on IFN-γ mAbs-coating plates, the spots were developed and were counted as IFN-γ-producing cells as described in Section 2 (ELISPOT). The numbers of IFN-γ-producing cells in monocyte-depleted PBMCs from the HS and CH groups were counted as described above. Horizontal bars represent median. HS, CH, as in Fig. 1.

3.4. Peripheral iNKT cells from chronic hepatitis C patients proliferate in response to αGalCer at a level comparable to those from healthy subjects

Next, we compared the ability of peripheral iNKT cells to proliferate in response to αGalCer-loaded DCs between the CH and the HS groups. In all subjects, the absolute number of iNKT cells was significantly

Table 2
Increase of iNKT cell numbers expanded with αGalCer-loaded Mo-DCs after 5 weeks of culture

	Healthy subjects (-fold)	Chronic hepatitis C patients (-fold)
Total iNKT cells	148 (21–2143)	249 (87–2220)
CD4+ iNKT cells	182 (3–630)	254 (45–2209)
CD4− iNKT cells	124 (1–5856)	319 (113–2277)

Data express median (range).

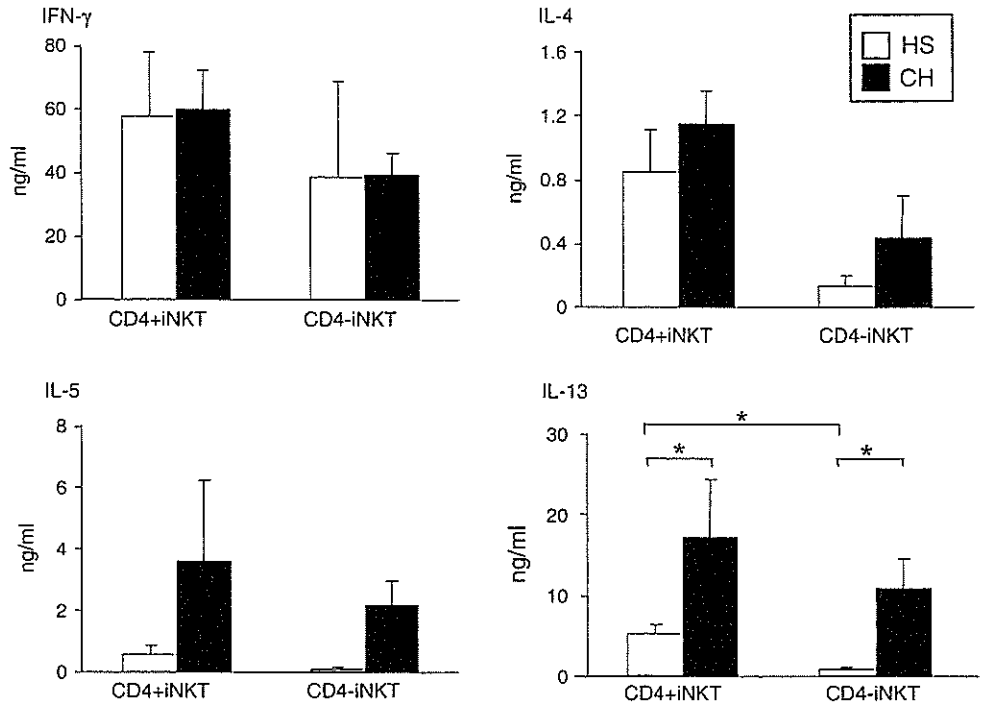

Fig. 4. Cytokine production from expanded iNKT cells stimulated with αGalCer-loaded Mo-DCs. Invariant NKT cells were expanded by culture with αGalCer-pulsed autologous Mo-DCs and subsequent cell sorting as described in Section 2. The activated iNKT cells were stimulated with αGalCer-pulsed allogeneic Mo-DCs for 24 h and the supernatants were collected for cytokine ELISA. The white column represents the healthy subject group and the black one represents the chronic hepatitis C group. The bars represent mean + SE of five different subjects. *$P < 0.05$ by Mann–Whitney U-test. HS, CH, as in Fig. 1.

increased after 5 weeks of culture. Although there was considerable variation among individuals in the proportion of iNKT cell increase (21–2220-fold), the total number of increased iNKT cells as well as their CD4 + or CD4− subsets in the CH group was comparable with those in the HS group (Table 2).

3.5. Expanded iNKT cells obtained from chronic hepatitis C patients produce more IL-13 in response to αGalCer than those from healthy subjects

In some reports, fresh isolated iNKT cells produce Th1 cytokines but not Th2 cytokines, while αGalCer-activated iNKT cells are able to produce both Th1 and Th2 cytokines [17,18]. Therefore, we compared the cytokine producing capacity of expanded iNKT cells. In contrast with the results of peripheral iNKT cells prior to in vitro expansion, the expanded iNKT cells produced considerable amounts of IL-4, IL-5 and IL-13 as well as IFN-γ in response to αGalCer (Fig. 4). The level of IFN-γ production from expanded iNKT cells did not differ between the CH and the HS groups, either from CD4 + or CD4− subsets (Fig. 4). With regard to Th2 cytokines, CD4 + iNKT cells in the HS produced significantly more IL-13 and tended to produce more IL-4 and IL-5 than the CD4− iNKT cells. In contrast, in the CH group, similar predominance of CD4 + iNKT cells over CD4− cells in Th2 cytokine production was observed, but did not reach a significant level. Of particular interest is the finding that a significantly larger amount of IL-13 was released from CD4 + as well as CD4− iNKT cells in the CH group as compared to those in the HS group (Fig. 4). A similar tendency was observed as the enhanced production of IL-4 and IL-5 from iNKT cells in the CH group. Thus, the activated iNKT cells obtained from chronic hepatitis C patients release more Th2-type cytokines, most significantly IL-13, than those from healthy subjects.

4. Discussion

Invariant NKT cells play distinctive roles in the regulation of immune responses in various diseases. In HIV infection, iNKT cells decrease in parallel with an increase in the viral load, which is due to direct HIV infection to these cells [11,13]. As for the frequency of peripheral iNKT cells in HCV infection, some conflicting results have been published. It has been reported that the number of iNKT cells in HCV-infected patients was in the same range as that in healthy subjects [15,16]. In contrast, other report showed that their number was

less in HCV viremic patients than non-viremic patients or healthy individuals [14]. In the present study, the frequencies of iNKT cells and their subsets in HCV-infected patients were comparable with those in healthy subjects. Several investigators reported that there are certain factors influencing iNKT cell numbers, such as gender and age in the study population [19,20]. Although no significant correlation was found between these background factors and iNKT cell frequency in our study, demographic as well as ethnic differences in the subjects might be involved in the discordant observations among these studies.

Limited numbers of peripheral iNKT cells have hampered the progress of research on the function of these cells. We used ELISPOT assay to analyze IFN-γ production from freshly isolated peripheral iNKT cells. The IFN-γ producing capacity of fresh peripheral iNKT cells from HCV-infected patients was comparable with those from healthy subjects. However, fresh iNKT cells produced negligible amounts of Th2 cytokines regardless of the presence or absence of HCV infection. Several investigators have reported that fresh iNKT cells are capable of predominantly producing Th1 cytokines compared to Th2 cytokines in response to αGalCer [17,18]. However, iNKT cells cultured with αGalCer are reported to gain the capacity to produce both Th1 and Th2 cytokines [17,18,21], implying that activated iNKT cells are able to secrete Th2 cytokines.

To analyze the capacity of cytokine production of activated iNKT cells, we thus expanded fresh iNKT cells with αGalCer-loaded DCs. However, the possibility remains that the experimental conditions may influence on iNKT cell functions, resulting in the functional difference between in vitro cultured iNKT cells and fresh iNKT cells in vivo. In the present study, the proliferative capacity of iNKT cells from HCV-infected patients was comparable with those from healthy donors, implying that expanded cells reflect the cell functions in vivo either in patients or donors. In clear contrast with fresh iNKT cells, the expanded iNKT cells from HCV-infected patients were able to produce a comparable amount of IFN-γ but more Th2 cytokines, most significantly IL-13, than those from healthy subjects. The mechanisms that induce Th2 bias of iNKT cells in HCV infection are yet to be demonstrated. Since iNKT cells were activated with αGalCer-pulsed autologous DCs, the functional alteration of DCs in HCV infection [22,23] may be responsible for the Th2 bias of activated iNKT cells.

With regard to the involvement of iNKT cells in the pathogenesis of chronic hepatitis C, several possibilities can be considered. First, Th2-biased iNKT cells may impede HCV clearance by suppressing the Th1 response. In this study, IL-13 production from expanded iNKT cells was not correlated with serum HCVRNA titres. However, IFN-γ from CD4+ iNKT cells tended to be inversely correlated with serum HCVRNA levels ($P = 0.07$, data not shown), while IL-4 from CD4− iNKT cells was positively correlated with HCVRNA quantity ($P = 0.07$, data not shown), suggesting an active role of iNKT cells in the control of HCV replication. Second, iNKT cells are involved in the progression of fibrosis in HCV-infected liver. Recently, other groups have reported that IL-4 and IL-13 from fresh iNKT cells were increased in liver cirrhosis caused by HBV or HCV, implying that these cells are profibrogenic to the liver [21,24,25]. If this is the case, the present study suggests that iNKT cells in chronic HCV infection are profibrogenic per se even in the pre-cirrhotic stage. Third, it is conceivable that the secretion of Th2 cytokines from iNKT cells is one of the compensatory mechanisms of liver inflammation. In patients with multiple sclerosis, a chronic inflammatory disease of the central nervous system, who are in remission, the iNKT cells produce a larger amount of IL-4 than those from patients in relapse [10], suggesting that iNKT cells may alleviate Th1-mediated inflammation by releasing Th2 cytokines. Analyses of liver-infiltrating lymphocytes in HCV-infected liver have disclosed that Th1-type CD4 T cells are compartmentalized [26], suggesting that the Th1 response is related to liver injury. Our study showed that CXCR3 expression on peripheral iNKT cells was higher in the CH group than those in the HS, whereas CCR7 or CD62L expressions were low in both groups. These results suggest that peripheral iNKT cells in HCV infection are prone to be of the tissue-infiltrating type, not the lymphoid-homing type. It has been reported that the expressions of IP-10 or MIG, which are ligands of CXCR3, are increased in HCV-infected liver, in correlation with the degree of inflammation [27–29]. Additionally, enhanced expression of CD1d is detected on the inflammatory infiltrates in HCV-infected liver [21,29,30]. Therefore, our results indicate the following hypothetical pathway of iNKT cell recruitment. Invariant NKT cells expressing CXCR3 tend to be mobilized in an inflamed liver, where they are activated via CD1d-expressing cells, and subsequently secrete large amount of Th2 cytokines.

Of particular importance is the large population of iNKT cells in liver-infiltrating lymphocytes compared to peripheral blood even in the steady state [31,32]. Thus, further examinations of liver-infiltrating iNKT cells are arguably necessary to understand the precise roles of iNKT cells in HCV-infected liver.

In summary, we demonstrated that the number and functions of peripheral iNKT cells from HCV-infected patients are comparable with those from healthy subjects at the steady state, but activated iNKT cells from patients released more Th2 cytokines, most significantly IL-13, than those from the controls. The altered functions of these cells in chronic hepatitis C may be involved in the pathogenesis of HCV-induced liver disease.

References

[1] Houghton M, Weiner A, Han J, Kuo G, Choo QL. Molecular biology of the hepatitis C viruses: implications for diagnosis, development and control of viral disease. Hepatology 1991;14:381–388.

[2] Diepolder HM, Zachoval R, Hoffmann RM, Wierenga EA, Santantonio T, Jung MC, et al. Possible mechanism involving T-lymphocyte response to non-structural protein 3 in viral clearance in acute hepatitis C virus infection. Lancet 1995;346:1006–1007.

[3] Cramp ME, Carucci P, Rossol S, Chokshi S, Maertens G, Williams R, et al. Hepatitis C virus (HCV) specific immune responses in anti-HCV positive patients without hepatitis C viraemia. Gut 1999;44:424–429.

[4] Godfrey DI, Hammond KJ, Poulton LD, Smyth MJ, Baxter AG. NKT cells: facts, functions and fallacies. Immunol Today 2000;21:573–583.

[5] Exley MA, Koziel MJ. To be or not to be NKT: natural killer T cells in the liver. Hepatology 2004;40:1033–1040.

[6] Kawano T, Cui J, Koezuka Y, Toura I, Kaneko Y, Motoki K, et al. CD1d-restricted and TCR-mediated activation of valpha14 NKT cells by glycosylceramides. Science 1997;278:1626–1629.

[7] Spada FM, Koezuka Y, Porcelli SA. CD1d-restricted recognition of synthetic glycolipid antigens by human natural killer T cells. J Exp Med 1998;188:1529–1534.

[8] Takahashi T, Chiba S, Nieda M, Azuma T, Ishihara S, Shibata Y, et al. Cutting edge: analysis of human V alpha 24 + CD8 + NK T cells activated by alpha-galactosylceramide-pulsed monocyte-derived dendritic cells. J Immunol 2002;168:3140–3144.

[9] Wilson SB, Kent SC, Patton KT, Orban T, Jackson RA, Exley M, et al. Extreme Th1 bias of invariant Valpha24JalphaQ T cells in type 1 diabetes. Nature 1998;391:177–181.

[10] Araki M, Kondo T, Gumperz JE, Brenner MB, Miyake S, Yamamura T. Th2 bias of CD4 + NKT cells derived from multiple sclerosis in remission. Int Immunol 2003;15:279–288.

[11] Sandberg JK, Fast NM, Palacios EH, Fennelly G, Dobroszycki J, Palumbo P, et al. Selective loss of innate CD4(+) V alpha 24 natural killer T cells in human immunodeficiency virus infection. J Virol 2002;76:7528–7534.

[12] Tahir SM, Cheng O, Shaulov A, Koezuka Y, Bubley GJ, Wilson SB, et al. Loss of IFN-gamma production by invariant NK T cells in advanced cancer. J Immunol 2001;167:4046–4050.

[13] Motsinger A, Haas DW, Stanic AK, Van Kaer L, Joyce S, Unutmaz D. CD1d-restricted human natural killer T cells are highly susceptible to human immunodeficiency virus 1 infection. J Exp Med 2002;195:869–879.

[14] Lucas M, Gadola S, Meier U, Young NT, Harcourt G, Karadimitris A, et al. Frequency and phenotype of circulating Valpha24/Vbeta11 double-positive natural killer T cells during hepatitis C virus infection. J Virol 2003;77:2251–2257.

[15] Karadimitris A, Gadola S, Altamirano M, Brown D, Woolfson A, Klenerman P, et al. Human CD1d-glycolipid tetramers generated by in vitro oxidative refolding chromatography. Proc Natl Acad Sci USA 2001;98:3294–3298.

[16] van der Vliet HJ, Molling JW, von Blomberg BM, Kolgen W, Stam AG, de Gruijl TD, et al. Circulating Valpha24(+)Vbeta11(+) NKT cell numbers and dendritic cell CD1d expression in hepatitis C virus infected patients. Clin Immunol 2005;114:183–189.

[17] Fujii S, Shimizu K, Steinman RM, Dhodapkar MV. Detection and activation of human Valpha24 + natural killer T cells using alpha-galactosyl ceramide-pulsed dendritic cells. J Immunol Methods 2003;272:147–159.

[18] Gumperz JE, Miyake S, Yamamura T, Brenner MB. Functionally distinct subsets of CD1d-restricted natural killer T cells revealed by CD1d tetramer staining. J Exp Med 2002;195:625–636.

[19] Sandberg JK, Bhardwaj N, Nixon DF. Dominant effector memory characteristics, capacity for dynamic adaptive expansion, and sex bias in the innate Valpha24 NKT cell compartment. Eur J Immunol 2003;33:588–596.

[20] DelaRosa O, Tarazona R, Casado JG, Alonso C, Ostos B, Pena J, et al. Valpha24 + NKT cells are decreased in elderly humans. Exp Gerontol 2002;37:213–217.

[21] de Lalla C, Galli G, Aldrighetti L, Romeo R, Mariani M, Monno A, et al. Production of profibrotic cytokines by invariant NKT cells characterizes cirrhosis progression in chronic viral hepatitis. J Immunol 2004;173:1417–1425.

[22] Kanto T, Hayashi N, Takehara T, Tatsumi T, Kuzushita N, Ito A, et al. Impaired allostimulatory capacity of peripheral blood dendritic cells recovered from hepatitis C virus-infected individuals. J Immunol 1999;162:5584–5591.

[23] Kanto T, Inoue M, Miyatake H, Sato A, Sakakibara M, Yakushijin T, et al. Reduced numbers and impaired ability of myeloid and plasmacytoid dendritic cells to polarize T helper cells in chronic hepatitis C virus infection. J Infect Dis 2004;190:1919–1926.

[24] Wynn TA. IL-13 effector functions. Annu Rev Immunol 2003;21:425–456.

[25] Kodera T, McGaha TL, Phelps R, Paul WE, Bona CA. Disrupting the IL-4 gene rescues mice homozygous for the tight-skin mutation from embryonic death and diminishes TGF-beta production by fibroblasts. Proc Natl Acad Sci USA 2002;99:3800–3805.

[26] Bertoletti A, D'Elios MM, Boni C, De Carli M, Zignego AL, Durazzo M, et al. Different cytokine profiles of intraphepatic T cells in chronic hepatitis B and hepatitis C virus infections. Gastroenterology 1997;112:193–199.

[27] Shields PL, Morland CM, Salmon M, Qin S, Hubscher SG, Adams DH. Chemokine and chemokine receptor interactions provide a mechanism for selective T cell recruitment to specific liver compartments within hepatitis C-infected liver. J Immunol 1999;163:6236–6243.

[28] Harvey CE, Post JJ, Palladinetti P, Freeman AJ, Ffrench RA, Kumar RK, et al. Expression of the chemokine IP-10 (CXCL10) by hepatocytes in chronic hepatitis C virus infection correlates with histological severity and lobular inflammation. J Leukoc Biol 2003;74:360–369.

[29] Apolinario A, Majano PL, Alvarez-Perez E, Saez A, Lozano C, Vargas J, et al. Increased expression of T cell chemokines and their receptors in chronic hepatitis C: relationship with the histological activity of liver disease. Am J Gastroenterol 2002;97:2861–2870.

[30] Durante-Mangoni E, Wang R, Shaulov A, He Q, Nasser I, Afdhal N, et al. Hepatic CD1d expression in hepatitis C virus infection and recognition by resident proinflammatory CD1d-reactive T cells. J Immunol 2004;173:2159–2166.

[31] Kawarabayashi N, Seki S, Hatsuse K, Ohkawa T, Koike Y, Aihara T, et al. Decrease of CD56(+)T cells and natural killer cells in cirrhotic livers with hepatitis C may be involved in their susceptibility to hepatocellular carcinoma. Hepatology 2000;32:962–969.

[32] Nuti S, Rosa D, Valiante NM, Saletti G, Caratozzolo M, Dellabona P, et al. Dynamics of intra-hepatic lymphocytes in chronic hepatitis C: enrichment for Valpha24 + T cells and rapid elimination of effector cells by apoptosis. Eur J Immunol 1998;28:3448–3455.

Differential roles of MDA5 and RIG-I helicases in the recognition of RNA viruses

Hiroki Kato[1,3]*, Osamu Takeuchi[1,3]*, Shintaro Sato[3], Mitsutoshi Yoneyama[4], Masahiro Yamamoto[1], Kosuke Matsui[1], Satoshi Uematsu[1], Andreas Jung[1], Taro Kawai[3], Ken J. Ishii[3], Osamu Yamaguchi[5], Kinya Otsu[5], Tohru Tsujimura[6], Chang-Sung Koh[7], Caetano Reis e Sousa[8], Yoshiharu Matsuura[2], Takashi Fujita[4] & Shizuo Akira[1,3]

The innate immune system senses viral infection by recognizing a variety of viral components (including double-stranded (ds)RNA) and triggers antiviral responses[1,2]. The cytoplasmic helicase proteins RIG-I (retinoic-acid-inducible protein I, also known as Ddx58) and MDA5 (melanoma-differentiation-associated gene 5, also known as Ifih1 or Helicard) have been implicated in viral dsRNA recognition[3–7]. *In vitro* studies suggest that both RIG-I and MDA5 detect RNA viruses and polyinosine-polycytidylic acid (poly(I:C)), a synthetic dsRNA analogue[3]. Although a critical role for RIG-I in the recognition of several RNA viruses has been clarified[8], the functional role of MDA5 and the relationship between these dsRNA detectors *in vivo* are yet to be determined. Here we use mice deficient in MDA5 (*MDA5*$^{-/-}$) to show that MDA5 and RIG-I recognize different types of dsRNAs: MDA5 recognizes poly(I:C), and RIG-I detects *in vitro* transcribed dsRNAs. RNA viruses are also differentially recognized by RIG-I and MDA5. We find that RIG-I is essential for the production of interferons in response to RNA viruses including paramyxoviruses, influenza virus and Japanese encephalitis virus, whereas MDA5 is critical for picornavirus detection. Furthermore, *RIG-I*$^{-/-}$ and *MDA5*$^{-/-}$ mice are highly susceptible to infection with these respective RNA viruses compared to control mice. Together, our data show that RIG-I and MDA5 distinguish different RNA viruses and are critical for host antiviral responses.

Host pattern recognition receptors, such as Toll-like receptors (TLRs) and helicase family members, have an essential role in the recognition of molecular patterns specific for different viruses, including DNA, single-stranded (ss)RNA, dsRNA and glycoproteins[1,9,10]. dsRNA can be generated during viral infection as a replication intermediate for RNA viruses. TLR3, which localizes in the endosomal membrane, has been shown to recognize viral dsRNA as well as the synthetic dsRNA analogue poly(I:C) (refs 11, 12). The cytoplasmic proteins RIG-I and MDA5 have also been identified as dsRNA detectors[3–5,7,13]. RIG-I and MDA5 contain two caspase-recruitment domains (CARDs) and a DExD/H-box helicase domain. RIG-I recruits a CARD-containing adaptor, IPS-1 (also known as MAVS, VISA or Cardif)[14–17]. IPS-1 relays the signal to the kinases TBK1 and IKK-i, which phosphorylate interferon-regulatory factor-3 (IRF-3) and IRF-7, transcription factors essential for the expression of type-I interferons[18–22]. In contrast, TLR3 activates TBK1 and IKK-i through the TIR-domain-containing adaptor TRIF (also known as Ticam1)[12].

In vitro studies have shown that both RIG-I and MDA5 can bind to poly(I:C) and respond to poly(I:C) and RNA viruses[6]. We have generated *RIG-I*$^{-/-}$ mice, and show that RIG-I is essential eliciting the immune responses against several RNA viruses, including Newcastle disease virus (NDV), Sendai virus (SeV) and vesicular stomatitis virus (VSV), in various cells except for plasmacytoid dendritic cells (pDCs)[8]. Hepatitis C virus and Japanese encephalitis virus are also reported to be recognized by RIG-I *in vitro*[23,24].

The *in vivo* functional relationship between RIG-I and MDA5 remains to be determined. To investigate a functional role for MDA5 *in vivo*, we generated *MDA5*$^{-/-}$ mice and investigated viral recognition (Supplementary Fig. 1). In contrast to *RIG-I*$^{-/-}$ mice, which are mostly embryonic lethal, *MDA5*$^{-/-}$ mice are born in a mendelian ratio, grow healthily and do not show gross developmental abnormalities until 24 weeks of age. Flow cytometric analysis of leukocytes from the spleen and lymph nodes (staining for CD3, B220 and CD11c) revealed that the composition of lymphocytes and dendritic cells is similar in wild-type and *MDA5*$^{-/-}$ mice (data not shown).

TLR3, RIG-I and MDA5 have been implicated in the recognition of poly(I:C) and the subsequent induction of antiviral responses. However, their exact contribution to *in vivo* responses against dsRNA has yet to be clarified. We therefore examined the *in vivo* responses to poly(I:C) in mice lacking RIG-I, MDA5 or TRIF, or both MDA5 and TRIF. Administration of poly(I:C) led to rapid induction of the cytokines interferon-α (IFN-α), IFN-β, interleukin-6 (IL-6) and IL-12 in sera of both wild-type and *RIG-I*$^{-/-}$ mice (Fig. 1a and Supplementary Fig. 2a). In contrast, *MDA5*$^{-/-}$ mice failed to produce IFN-α and IFN-β in response to poly(I:C), and production of IL-6 and IL-12p40 was also significantly impaired (Fig. 1b). Although *Trif*$^{-/-}$ mice produced normal amounts of IFN-α, they also showed severely impaired production of IL-12p40 and partial impairment in IL-6 production. *MDA5*$^{-/-}$; *Trif*$^{-/-}$ double-knockout mice failed to induce IFN-α, IL-6 and IL-12p40 in response to poly(I:C). These results indicate that MDA5 is essential for poly(I:C)-induced IFN-α production and TLR3 signalling is critical for IL-12 production, whereas both MDA5 and TLR3 regulate IL-6 production.

[1]Department of Host Defense, [2]Department of Molecular Virology, Research Institute for Microbial Diseases, Osaka University, and [3]ERATO, Japan Science and Technology Agency, 3-1 Yamada-oka, Suita, Osaka 565-0871, Japan. [4]Department of Genetics and Molecular Biology, Institute for Virus Research, Kyoto University, 53 Kawahara-cho, Shogoin, Sakyo-ku, Kyoto 606-8507, Japan. [5]Department of Cardiovascular Medicine, Osaka University Graduate School of Medicine, 2-2 Yamada-oka, Suita, Osaka 565-0871, Japan. [6]Department of Pathology, Hyogo College of Medicine, 1-1 Mukogawa-cho, Nishinomiya, Hyogo 663-8501, Japan. [7]Department of Medical Technology, Shinshu University School of Allied Medical Sciences, 3-1-1 Asahi, Matsumoto 390-8621, Japan. [8]Immunobiology Laboratory, Cancer Research UK London Research Institute, Lincoln's Inn Fields Laboratories, 44 Lincoln's Inn Fields, London WC2A 3PX, UK.
*These authors contributed equally to this work.

When bone-marrow-derived dendritic cells generated by granulocyte–macrophage colony-stimulating factor (GMCSF) were incubated in the presence of poly(I:C), production of IFN-α and IFN-β was severely impaired in *MDA5*$^{-/-}$, but not in *RIG-I*$^{-/-}$ or *Trif*$^{-/-}$, GMCSF-DCs (Fig. 1c and Supplementary Fig. 2b). Even when poly(I:C) was transfected into GMCSF-DCs using lipofectamine, poly(I:C) induced IFN-β production in an MDA5-dependent, but not a RIG-I- or TRIF-dependent, manner (Fig. 1d). IFN-β production in response to poly(I:C) was also impaired in *MDA5*$^{-/-}$ mouse embryonic fibroblasts (MEFs) (Fig. 1e), indicating that poly(I:C) is primarily recognized by MDA5, not RIG-I and TLR3, in these cells.

dsRNAs transcribed *in vitro* (Supplementary Fig. 2c) also stimulated MEFs to produce IFN-β. Unlike for poly(I:C), wild-type and *MDA5*$^{-/-}$ MEFs produced comparable amounts of IFN-β (Fig. 1e) in response to *in vitro* transcribed dsRNAs. In contrast, *RIG-I*$^{-/-}$ MEFs did not produce detectable amounts of IFN-β, indicating that RIG-I is essential for the detection of *in vitro* transcribed dsRNAs. As RIG-I, but not MDA5, is responsible for IFN-β production in response to dsRNAs of various lengths, these helicases probably distinguish nucleotide structure or sequence, but not length. Together, these results indicate that MDA5 and RIG-I are involved in the detection of poly(I:C) and *in vitro* transcribed dsRNAs, respectively.

This finding led us to hypothesize that RIG-I and MDA5 are involved in the detection of different RNA viruses. We have previously shown that a set of negative-sense RNA viruses are recognized by RIG-I[8]. We first examined IFN-β and IFN-α production in *MDA5*$^{-/-}$ MEFs in response to a set of negative-sense ssRNA viruses, including NDV, SeV, VSV and influenza virus. As infection with most of the wild-type viruses (except NDV) failed to induce type-I interferons in MEFs, owing to suppression of interferon responses by viral proteins (data not shown), we also used mutant viruses lacking viral interferon-inhibitory proteins. As shown in Fig. 2a and Supplementary Fig. 4b, wild-type MEFs produce IFN-β and IFN-α in response to these mutant viruses. Production of type-I interferons was severely impaired in *RIG-I*$^{-/-}$ MEFs compared to wild-type cells, but MDA5 was dispensable for the production of type-I interferons. Japanese encephalitis virus (JEV), a positive-sense ssRNA virus belonging to the flavivirus family, also required RIG-I, but not MDA5, for IFN-β production (Fig. 2b).

We then examined the interferon responses of MEFs to encephalomyocarditis virus (EMCV), a positive-sense ssRNA virus belonging to the picornavirus family. EMCV-induced IFN-β production was abrogated in *MDA5*$^{-/-}$ MEFs (Fig. 2c). In contrast, wild-type and *RIG-I*$^{-/-}$ MEFs produced comparable amounts of IFN-β, indicating that EMCV is specifically recognized by MDA5. The induction of genes encoding IFN-β, IP-10 and IL-6 in response to EMCV was abrogated in *MDA5*$^{-/-}$ macrophages (Supplementary Fig. 3d). The synthesis of cellular proteins in *MDA5*$^{-/-}$ MEFs was progressively inhibited during EMCV infection, to an extent and with kinetics similar to wild-type MEFs (Supplementary Fig. 5), indicating that the EMCV infection was established in wild-type and *MDA5*$^{-/-}$ MEFs in a similar manner. Moreover, other viruses belonging to the picornavirus family (Theiler's and Mengo viruses) also induced IFN-α through MDA5 (Supplementary Fig. 4d). Furthermore, the production of IFN-β in response to SeV and EMCV was impaired in *RIG-I*$^{-/-}$ and *MDA5*$^{-/-}$ GMCSF-DCs, respectively (Fig. 2d, e), indicating that conventional dendritic cells (cDCs) also use these helicases for the differential recognition of viruses. EMCV-induced production of IL-6 was also abrogated in *MDA5*$^{-/-}$, but not *RIG-I*$^{-/-}$, cDCs (Supplementary Fig. 4c). Therefore, MDA5 is critical for the regulation of pro-inflammatory cytokines as well as type-I interferons in response to EMCV.

We next examined whether viral RNAs derived from VSV and EMCV recapitulate the production of interferons through MDA5 and RIG-I. When transfected into GMCSF-DCs by lipofection, RNAs prepared from VSV or EMCV induced production of IFN-α in a RIG-I- or MDA5-dependent manner, respectively (Fig. 2f). We also performed reconstitution experiments by transfecting RIG-I or MDA5 expression vectors into *RIG-I*$^{-/-}$; *MDA5*$^{-/-}$ MEFs, in which IFN-β induction was completely abrogated in response to infection with EMCV or SeV Cm (SeV with a mutated C protein) (Fig. 2g). The ectopic expression of human RIG-I, but not MDA5, activated the *Ifnb* promoter in response to SeV Cm. Reciprocally, cells expressing human MDA5, but not RIG-I, activated the *Ifnb* promoter in response to EMCV in a dose-dependent manner (Fig. 2h). These results indicate that human RIG-I and MDA5 recognize different RNA viruses by recognizing viral RNAs.

Previous studies have shown that pDCs use mainly the TLR system instead of RIG-I in the recognition of several RNA viruses[8]. MyD88 is an adaptor protein essential for TLR signalling (except through TLR3). We purified B220^{+} pDCs from Flt3L-generated bone-marrow-derived dendritic cells (Flt3L-DCs) and infected them with EMCV. pDCs from *Myd88*$^{-/-}$, but not *MDA5*$^{-/-}$, mice showed a profound defect in IFN-α production (Supplementary Fig. 6). Reciprocally, MDA5, but not MyD88, is required for the production of IFN-α in B220^{-} cDCs purified from Flt3L-DCs (Supplementary Fig. 6). These results indicate that both MDA5 and RIG-I are

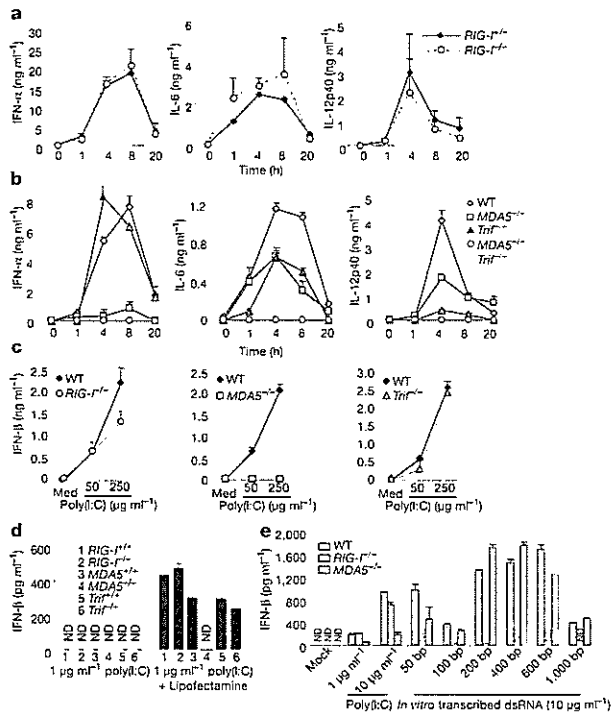

Figure 1 | Roles of MDA5, RIG-I and TRIF in the recognition of synthesized dsRNAs and dsRNA analogues. **a**, **b**, *RIG-I*$^{-/-}$ and littermate *RIG-I*$^{+/-}$ mice (**a**) or wild-type (WT), *MDA5*$^{-/-}$, *Trif*$^{-/-}$ or *MDA5*$^{-/-}$; *Trif*$^{-/-}$ double-knockout mice (**b**) were injected intravenously with 200 μg poly(I:C) for the indicated periods, and IFN-α, IL-6 and IL-12p40 production was measured in serum by ELISA. Data show mean ± s.d. **c**, GMCSF-DCs from *RIG-I*$^{-/-}$, *MDA5*$^{-/-}$, *TRIF*$^{-/-}$ and littermate control mice were incubated in the presence of 50 or 250 μg ml^{-1} poly(I:C) for 24 h. IFN-β production in the cell culture supernatants was measured by ELISA. Med, medium only. **d**, GMCSF-DCs were treated with 1 μg ml^{-1} poly(I:C) complexed with or without lipofectamine 2000 for 24 h, and IFN-β production was measured. **e**, Wild-type, *RIG-I*$^{-/-}$ and *MDA5*$^{-/-}$ MEFs were treated with poly(I:C) or *in vitro* transcribed dsRNAs of indicated lengths complexed with lipofectamine 2000 for 12 h, and IFN-β production was measured. Error bars indicate s.d. of triplicate wells in a single experiment; data are representative of three independent experiments. ND, not detected.

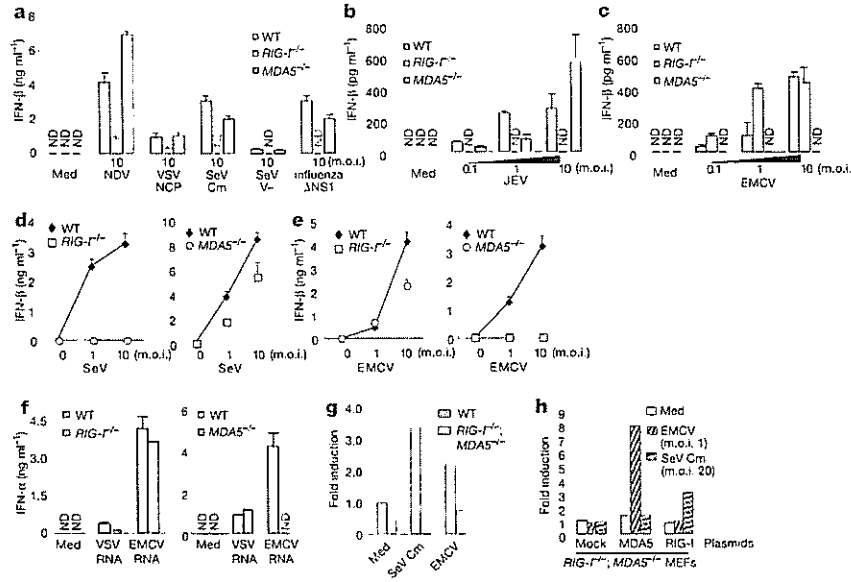

Figure 2 | Differential viral recognition by RIG-I and MDA5. **a**, Wild-type, *RIG-I*$^{-/-}$ and *MDA5*$^{-/-}$ MEFs were exposed to negative-sense ssRNA viruses, including NDV, VSV lacking a variant of M protein (NCP), SeV with a mutated C protein (Cm), SeV lacking V protein (V^{-}), and influenza virus lacking the NS1 protein (ΔNS1) for 24 h. IFN-β production in the culture supernatants was measured by ELISA. **b**, **c**, Wild-type, *RIG-I*$^{-/-}$ and *MDA5*$^{-/-}$ MEFs were exposed to the positive-sense ssRNA viruses JEV (**b**) and EMCV (**c**), and IFN-β production was measured. **d**, **e**, GMCSF-DCs from *RIG-I*$^{-/-}$ and *MDA5*$^{-/-}$ mice and their littermate wild-type mice were infected with an increasing m.o.i. of SeV V^{-} (**d**) or EMCV (**e**) for 24 h, and IFN-β production was measured. **f**, Wild-type, *RIG-I*$^{-/-}$ and *MDA5*$^{-/-}$ GMCSF-DCs were treated with RNAs directly prepared from VSV and EMCV (complexed with lipofectamine 2000) for 24 h, and IFN-α production was measured. **g**, Wild-type and *RIG-I*$^{-/-}$; *MDA5*$^{-/-}$ MEFs were transiently transfected with a reporter construct containing the *Ifnb* promoter and exposed to SeV Cm or EMCV for 24 h. Cell lysates were then prepared and subjected to a luciferase assay. **h**, RIG-I$^{-/-}$; MDA5$^{-/-}$ MEFs were transiently transfected with the *Ifnb* promoter construct together with expression plasmids encoding human RIG-I or MDA5. The cells were then infected with EMCV or SeV Cm for 24 h and were subjected to a luciferase assay. Error bars in **a**–**g** indicate s.d. of triplicate wells in a single experiment; data are representative of three independent experiments. ND, not detected.

dispensable for the viral induction of IFN-α in pDCs.

We next examined the *in vivo* roles of MDA5 and RIG-I in host defence against viral infection. Although most *RIG-I*$^{-/-}$ mice are embryonic lethal[8], we could efficiently obtain live adult mice by intercrossing the *RIG-I*$^{+/-}$ mice obtained after *RIG-I*$^{+/-}$ × ICR crosses (Supplementary Table 1). When the mice were infected with JEV, serum IFN-α levels were markedly decreased in *RIG-I*$^{-/-}$ mice compared to littermate *RIG-I*$^{+/-}$ mice. In contrast, *MDA5*$^{-/-}$ mice did not show a defect in JEV-induced systemic IFN-α production (Fig. 3a). IFN-α production was partially impaired in *Myd88*$^{-/-}$ mice compared to wild-type mice, but the extent of this impairment was far less than in *RIG-I*$^{-/-}$ mice (Fig. 3a). These data suggest that the TLR system is not critical for the induction of serum IFN-α *in vivo* in response to JEV. Consistent with this finding, *RIG-I*$^{-/-}$ mice, but not *MDA5*$^{-/-}$ or *Myd88*$^{-/-}$ mice, were more susceptible to JEV infection than control mice (Fig. 3b). Furthermore, *RIG-I*$^{-/-}$ mice, but not *MDA5*$^{-/-}$ mice, succumbed to VSV infection, consistent with abrogated interferon responses (Supplementary Fig. 7). Thus, RIG-I-mediated recognition of a specific set of viruses has a critical role in antiviral host defence *in vivo*.

We next challenged the mice with EMCV as a model virus that is recognized by MDA5. Induction of IFN-β, IFN-α, RANTES and IL-6 was severely impaired in the sera of *MDA5*$^{-/-}$ mice (Fig. 4a and Supplementary Fig. 8). *MDA5*$^{-/-}$ mice and mice null for the IFN-α/β receptor (*Ifnar1*$^{-/-}$) were highly susceptible to EMCV infection (viral titre of 1×10^2 plaque-forming units (p.f.u.)) compared to littermate controls ($P < 0.01$) (Fig. 4b). In contrast, deficiency of neither RIG-I nor TLR3 affected the survival of mice infected with EMCV. Consistent with a previous report[22], *Myd88*$^{-/-}$ mice were modestly susceptible to EMCV infection compared to wild-type mice, implying that pDC-mediated responses are not critical for eliminating EMCV (Fig. 4b).

It is known that EMCV preferentially infects cardiomyocytes and causes myocarditis. Consistent with increased susceptibility to EMCV, viral titre in the heart was much higher in *MDA5*$^{-/-}$ mice compared to control mice (Fig. 4c). Histological analysis of hearts two days after EMCV infection revealed that focal necrosis of

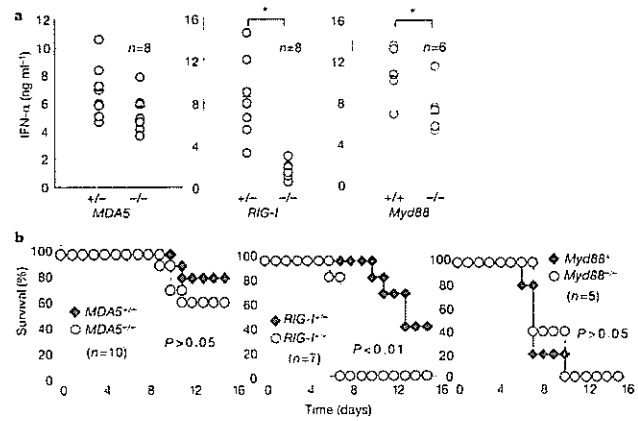

Figure 3 | Susceptibility of *RIG-I*$^{-/-}$ and *MDA5*$^{-/-}$ mice to JEV infection. **a**, *RIG-I*$^{+/-}$, *RIG-I*$^{-/-}$, *MDA5*$^{-/-}$ and *MDA5*$^{-/-}$ mice ($n = 8$), and *Myd88*$^{+/+}$ or *Myd88*$^{-/-}$ mice ($n = 6$), were injected intravenously with 2×10^7 p.f.u. JEV. Sera were collected 24 h after injection, and IFN-α production levels measured by ELISA. Circles represent individual mice, bars indicate mean values. Asterisk, $P < 0.05$ versus controls (*t*-test). **b**, The survival of 6-week-old mice (genotypes as indicated) infected intravenously with 2×10^7 p.f.u. JEV. Mice were monitored for 15 days ($P < 0.01$ between *RIG-I*$^{-/-}$ mice and their littermate controls, generalized Wilcoxon test).

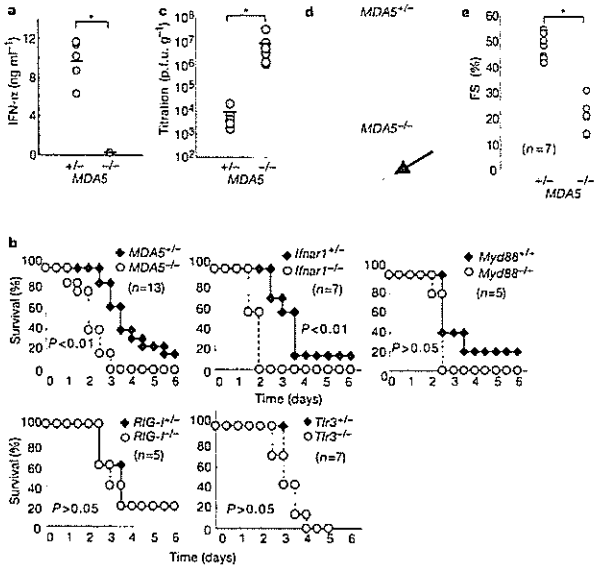

Figure 4 | Role of MDA5 in host defence against EMCV infection. **a**, $MDA5^{+/-}$ and $MDA5^{-/-}$ mice ($n = 5$) were inoculated intravenously with 1×10^7 p.f.u. EMCV. Sera were prepared 4 h after injection and IFN-α production levels determined by ELISA. **b**, The survival of 6-week-old mice (genotypes as indicated) infected with 1×10^2 p.f.u. EMCV intraperitoneally was monitored every 12 h for six days ($P < 0.01$ between $MDA5^{-/-}$ or $Ifnar1^{-/-}$ mice and their littermate controls, generalized Wilcoxon test). **c**, $MDA5^{+/-}$ and $MDA5^{-/-}$ mice were infected intraperitoneally with 1×10^2 p.f.u. EMCV. After 48 h, mice were killed and virus titres in hearts were determined by plaque assay. **d**, Heart sections of $MDA5^{+/-}$ and $MDA5^{-/-}$ mice, two days after infection, were assessed for histological changes using haematoxylin and eosin staining. Arrow indicates the focal necrosis of cardiomyocytes. **e**, Cardiac function of mice 48 h after EMCV infection was assessed by echocardiography (see Supplementary Fig. 8b). The fractional shortening (FS) after infection determined by transthoracic M-mode echocardiographic tracings is shown. Asterisk, $P < 0.05$ versus $MDA5^{+/-}$ mice (*t*-test).

cardiomyocytes had developed in $MDA5^{-/-}$ mice, but wild-type hearts showed no histological abnormalities at this time point (Fig. 4d). Notably, no infiltration of immune cells was observed in either wild-type or $MDA5^{-/-}$ heart sections at this time point. However, when cardiac performance was analysed by echocardiography two days after infection (Fig. 4e), cardiac contractility was severely depressed in $MDA5^{-/-}$ mice (fractional shortening 48.2 ± 4.9% in $MDA5^{+/-}$ mice, 21.2 ± 5.8% in $MDA5^{-/-}$ mice), indicating that $MDA5^{-/-}$ mice developed severe heart failure due to virus-induced cardiomyopathy. Thus, MDA5-mediated recognition of EMCV is a prerequisite for triggering antiviral responses as well as for prevention of myocardial dysfunction.

Together, our results demonstrate that RIG-I and MDA5 have essential roles in the recognition of different groups of RNA viruses, as well as in the subsequent production of type-I interferons and pro-inflammatory cytokines. We have found that poly(I:C) and *in vitro* transcribed dsRNA are recognized by MDA5 and RIG-I, respectively; this is in contrast to results from previous *in vitro* studies. RIG-I probably recognizes dsRNA generated over the course of RNA virus replication, as all *in vitro* transcribed dsRNAs tested except for poly(I:C) induced type-I interferons through RIG-I. In contrast, the endogenous ligand of MDA5 remains enigmatic. Moreover, how RIG-I and MDA5 differentially recognize natural dsRNAs is undetermined. Given that the helicase domains of RIG-I and MDA5 bind to dsRNA, analyses of the crystal structures of these domains should to help achieve a better understanding of the molecular mechanisms underlying this differential recognition. Furthermore, it is still possible that unknown dsRNA-binding proteins also function as direct receptors for viral RNAs.

Finally, the picornavirus family contains several viruses that are pathogenic for humans, including poliovirus, rhinovirus and the virus causing foot-and-mouth-disease. Our studies suggest that human MDA5 and RIG-I also recognize RNA viruses. Thus, identification of therapeutic agents that modify RIG-I or MDA5 may lead to antiviral strategies against selected viruses.

METHODS

Mice, cells and reagents. The generation of $MDA5^{-/-}$ mice is described in the Supplementary Information. $Myd88^{-/-}$, $Tlr3^{-/-}$ and $Trif^{-/-}$ mice have been described previously[12]. $Ifnar1^{-/-}$ mice have also been described previously[25]. $RIG\text{-}I^{+/-}$ mice in a 129Sv × C57BL/6 background were crossed with ICR mice, and the resulting $RIG\text{-}I^{+/-}$ mice were further intercrossed. Interbreeding of these $RIG\text{-}I^{+/-}$ mice produced healthy and fertile $RIG\text{-}I^{-/-}$ offspring, although their number was less than half that of $RIG\text{-}I^{+/+}$ progeny (Supplementary Table 1). $RIG\text{-}I^{-/-}$ and $RIG\text{-}I^{+/-}$ littermate mice were used for *in vivo* experiments. $RIG\text{-}I^{-/-}$; $MDA5^{-/-}$ mice in a 129Sv × C57BL/6 background were lethal at embryonic day 12.5. Additional details regarding cells, reagents and the preparation of *in vitro* transcribed dsRNA are provided in the Supplementary Information.

Viruses. NDV (ref. 3), VSV, VSV lacking a variant of M protein (NCP) (ref. 8), influenza virus lacking the NS1 protein (ΔNS1) (ref. 26), JEV (ref. 27) and EMCV (ref. 3) have been described previously. SeV and SeV lacking the V protein (V^-) or with mutated C proteins (Cm) were provided by A. Kato[28].

Luciferase assay. Wild-type or $RIG\text{-}I^{-/-}$; $MDA5^{-/-}$ MEFs were transiently transfected with a reporter construct containing the *Ifnb* promoter together with an empty vector (mock), or *RIG-I* or *MDA5* expression vectors. As an internal control, a *Renilla* luciferase construct was transfected. Transfected cells were untreated or infected with EMCV or SeV Cm (m.o.i. 20) for 24 h. The cells were lysed and subjected to a luciferase assay using a dual-luciferase reporter assay system (Promega) according to the manufacturer's instructions.

Analysis of mice after EMCV infection. Methods for plaque assays, histological analysis and echocardiography are described in the Supplementary Information.

Measurement of cytokine production. Cell culture supernatants were collected and analysed for IFN-β, IFN-α, IL-6 or IL-12p40 production using enzyme-linked immunosorbent assays (ELISAs). ELISA kits for mouse IFN-α and IFN-β were purchased from PBL Biomedical Laboratories, and those for IL-6, IL-12p40 and RANTES were obtained from R&D Systems.

Statistical analysis. Kaplan–Meier plots were constructed and a generalized Wilcoxon test was used to test for differences in survival between control and mutant mice after viral infection. Statistical significance of any differences in cytokine concentration and ECMV titres was determined using Student's *t*-tests.

Received 30 January; accepted 20 March 2006.
Published online 9 April 2006.

1. Akira, S., Uematsu, S. & Takeuchi, O. Pathogen recognition and innate immunity. *Cell* 124, 783–801 (2006).
2. Katze, M. G., He, Y. & Gale, M. Jr. Viruses and interferon: A fight for supremacy. *Nature Rev. Immunol.* 2, 675–687 (2002).
3. Yoneyama, M. *et al.* The RNA helicase RIG-I has an essential function in double-stranded RNA-induced innate antiviral responses. *Nature Immunol.* 5, 730–737 (2004).
4. Kang, D. C. *et al. mda-5*: An interferon-inducible putative RNA helicase with double-stranded RNA-dependent ATPase activity and melanoma growth-suppressive properties. *Proc. Natl Acad. Sci. USA* 99, 637–642 (2002).
5. Andrejeva, J. *et al.* The V proteins of paramyxoviruses bind the IFN-inducible RNA helicase, mda-5, and inhibit its activation of the *IFN-β* promoter. *Proc. Natl Acad. Sci. USA* 101, 17264–17269 (2004).
6. Yoneyama, M. *et al.* Shared and unique functions of the DExD/H-box helicases RIG-I, MDA5, and LGP2 in antiviral innate immunity. *J. Immunol.* 175, 2851–2858 (2005).
7. Rothenfusser, S. *et al.* The RNA helicase Lgp2 inhibits TLR-independent sensing of viral replication by retinoic acid-inducible gene-I. *J. Immunol.* 175, 5260–5268 (2005).
8. Kato, H. *et al.* Cell type-specific involvement of RIG-I in antiviral response. *Immunity* 23, 19–28 (2005).
9. Iwasaki, A. & Medzhitov, R. Toll-like receptor control of the adaptive immune responses. *Nature Immunol.* 5, 987–995 (2004).
10. Beutler, B. Inferences, questions and possibilities in Toll-like receptor signalling. *Nature* 430, 257–263 (2004).
11. Alexopoulou, L., Holt, A. C., Medzhitov, R. & Flavell, R. A. Recognition of double-stranded RNA and activation of NF-κB by Toll-like receptor 3. *Nature* 413, 732–738 (2001).

12. Yamamoto, M. *et al.* Role of adaptor TRIF in the MyD88-independent toll-like receptor signaling pathway. *Science* 301, 640–643 (2003).
13. Kovacsovics, M. *et al.* Overexpression of Helicard, a CARD-containing helicase cleaved during apoptosis, accelerates DNA degradation. *Curr. Biol.* 12, 838–843 (2002).
14. Kawai, T. *et al.* IPS-1, an adaptor triggering RIG-I- and Mda5-mediated type I interferon induction. *Nature Immunol.* 6, 981–988 (2005).
15. Seth, R. B., Sun, L., Ea, C. K. & Chen, Z. J. Identification and characterization of MAVS, a mitochondrial antiviral signaling protein that activates NF-κB and IRF 3. *Cell* 122, 669–682 (2005).
16. Xu, L. G. *et al.* VISA is an adapter protein required for virus-triggered IFN-β signaling. *Mol. Cell* 19, 727–740 (2005)
17. Meylan, E. *et al.* Cardif is an adaptor protein in the RIG-I antiviral pathway and is targeted by hepatitis C virus. *Nature* 437, 1167–1172 (2005).
18. Fitzgerald, K. A. *et al.* IKKε and TBK1 are essential components of the IRF3 signaling pathway. *Nature Immunol.* 4, 491–496 (2003).
19. Sharma, S. *et al.* Triggering the interferon antiviral response through an IKK-related pathway. *Science* 300, 1148–1151 (2003).
20. Hemmi, H. *et al.* The roles of two IκB kinase-related kinases in lipopolysaccharide and double stranded RNA signaling and viral infection. *J. Exp. Med.* 199, 1641–1650 (2004).
21. Sato, M. *et al.* Distinct and essential roles of transcription factors IRF-3 and IRF-7 in response to viruses for IFN-α/β gene induction. *Immunity* 13, 539–548 (2000).
22. Honda, K. *et al.* IRF-7 is the master regulator of type-I interferon-dependent immune responses. *Nature* 434, 772–777 (2005).
23. Chang, T. H., Liao, C. L. & Lin, Y. L. Flavivirus induces interferon-beta gene expression through a pathway involving RIG-I-dependent IRF-3 and PI3K-dependent NF-κB activation. *Microbes Infect.* 8, 157–171 (2006).
24. Melchjorsen, J. *et al.* Activation of innate defense against a paramyxovirus is mediated by RIG-I and TLR7 and TLR8 in a cell-type-specific manner. *J. Virol* 79, 12944–12951 (2005).
25. Hoshino, K., Kaisho, T., Iwabe, T., Takeuchi, O. & Akira, S. Differential involvement of IFN-β in Toll-like receptor-stimulated dendritic cell activation *Int. Immunol.* 14, 1225–1231 (2002).
26. Diebold, S. S., Kaisho, T., Hemmi, H., Akira, S. & Reis e Sousa, C. Innate antiviral responses by means of TLR7-mediated recognition of single-stranded RNA. *Science* 303, 1529–1531 (2004).
27. Mori, Y. *et al.* Nuclear localization of Japanese encephalitis virus core protein enhances viral replication. *J. Virol.* 79, 3448–3458 (2005).
28. Kato, A. *et al.* Characterization of the amino acid residues of sendai virus C protein that are critically involved in its interferon antagonism and RNA synthesis down-regulation. *J. Virol.* 78, 7443–7454 (2004).

Supplementary Information is linked to the online version of the paper at www.nature.com/nature.

Acknowledgements We thank all colleagues in our laboratory, K. Takeda, T. Shioda, E. Nakayama and K. Kiyotani for helpful discussions, A. Kato, T. Abe, Y. Mori, B. S. Kim and A. Palmenberg for viruses and plasmids, M. Hashimoto for secretarial assistance, and Y. Fujiwara, M. Shiokawa, N. Kitagaki and A. Shibano for technical assistance. This work was supported by grants from the Ministry of Education, Culture, Sports, Science and Technology in Japan, and from the 21st Century Center of Excellence Program of Japan.

Author Information Reprints and permissions information is available at npg.nature.com/reprintsandpermissions. The authors declare no competing financial interests. Correspondence and requests for materials should be addressed to S.A. (sakira@biken.osaka-u.ac.jp).

Available online at www.sciencedirect.com

ScienceDirect

Hepatology Research 35 (2006) 250–255

HEPATOLOGY RESEARCH

http://www.elsevier.com/locate/hepres

Immune responses of liver-infiltrating lymphocytes and peripheral blood mononuclear cells to hepatitis C virus core and NS3 antigens

Morihiro Tajimi [a,*], Takuhiro Ugajin [a], Masahiro Ota [b], Kazumasa Hiroishi [c], Ikuo Nakamura [a], Michio Imawari [c]

[a] *Division of Gastroenterology, Omiya Medical Center, Jichi Medical School, Japan*
[b] *Division of Pathology, Omiya Medical Center, Jichi Medical School, Japan*
[c] *Second Department of Internal Medicine, Showa University School of Medicine, Japan*

Received 20 February 2006; received in revised form 25 April 2006; accepted 28 April 2006
Available online 12 June 2006

Abstract

Background and aim: Th1/Th2 cytokine balance is thought to play an important role in antiviral immunity and pathogenesis in viral infection. Ex vivo hepatitis C virus (HCV) antigen-specific T-cell responses were investigated.
Methods: Using enzyme-linked immunospot assay, HCV core and NS3 antigen-specific interferon-γ-, interleukin-4- and interleukin-10-secreting cells were enumerated in peripheral blood mononuclear cells (PBMCs) from 30 chronic hepatitis C patients and 16 healthy controls, and in liver-infiltrating lymphocytes (LILs) from 17 of the 30 patients.
Results: IFN-γ- and IL-10-secreting cells in response to stimulation with HCV core and NS3 antigen were detectable in both PBMCs and LILs from patients with chronic hepatitis C, although frequencies of the cytokine-secreting cells were much higher in LILs than PBMCs. They were not detectable in PBMCs of healthy controls except for IL-10-secreting cells in response to HCV NS3 antigen stimulation. IL-4-secreting cells were hardly detectable in both PBMC and LIL in both the patients and the healthy controls. Frequencies of HCV NS3 antigen-specific IFN-γ- and IL-10-secreting cells in PBMCs correlated with those in LILs ($\rho = 0.599$, $p = 0.044$ and $\rho = 0.716$, $p = 0.004$, respectively).
Conclusions: These data provide further evidence of the immunomodulatory role of the $CD4^+CD25^+$ regulatory T lymphocytes in chronic HCV infection.

Keywords: Chronic hepatitis C; Hepatitis C virus infection; Enzyme-linked immunospot assay; Interferon-γ; Interleukin-4; Interleukin-10

1. Introduction

Chronic hepatitis C virus (HCV) infection is one of the major cause of chronic liver disease worldwide [1]; approximately 170 million people in the world are infected with HCV, the many of them have chronic hepatitis and will develop liver cirrhosis. As HCV mutate at a high frequency, host humoral immune responses to HCV may not be able to clear the virus [2,3].

Many studies suggested that cellular immune responses play a crucial role in both host defenses against viral infection and its immunopathogenesis. In acute and chronic HCV infection, HCV antigen-specific T-cell responses are thought to be important in clearance of the virus [4–13]. HCV antigen-specific liver infiltrating T lymphocytes are thought to be particularly important. Various studies have been conducted on host immune responses to HCV antigens using peripheral blood mononuclear cells (PBMCs). Although several studies have used liver-infiltrating lymphocytes (LILs), most of these LILs were first expanded using interleukin-2 (IL-2) because of its limited number obtained from a small specimen [14–17].

A key feature of the methods in the present study was the use of non-expanded LILs in enzyme-linked immunospot

* Corresponding author at: Division of Gastroenterology, Omiya Medical Center, Jichi Medical School, 1-847, Amanuma-tyo, Omiya-ku, Saitama 330-8503, Japan. Tel.: +81 48 647 2111; fax: +81 48 648 5188.
E-mail address: mtajimi@sowa-chuo.com (M. Tajimi).

1386-6346/$ – see front matter © 2006 Elsevier Ireland Ltd. All rights reserved.
doi:10.1016/j.hepres.2006.04.015

(ELISpot) assays to observe actual immune states at inflammatory sites. We also sought to confirm the validity of use of PBMCs to study host immune responses to HCV antigens, by comparing immune reactions of PBMCs to HCV antigens with those of LILs to HCV antigens.

Currently immunity to infection is thought to be controlled by distinct type 1 (Th1) and type 2 (Th2) subpopulations of T cells, as discriminated on the basis of cytokine secretion and function. In the present study, we determined secretion of IFN-γ, IL-4 and IL-10 by LILs and PBMCs in response to HCV core and NS3 antigens using ELISpot assay to clarify the role of Th1, Th2 cells in chronic HCV infection.

2. Materials and methods

2.1. Patients and controls

Table 1 shows the characteristics of patients and healthy controls studied. Patients with chronic hepatitis C were admitted to Omiya Medical Center, Jichi Medical School for diagnostic and therapeutic purposes between 1 April 1998 and 31 August 2000. Liver tissue samples from 17 patients were used to isolate liver-infiltrating lymphocytes. The liver biopsies and the PBMCs were obtained prior to interferon therapy. Of the 30 patients, 26 were treated with 6–10 million units of interferon-α daily for the first 2 weeks, followed by injection of the same dose of IFN-α three times weekly for the following 22 weeks. Serum HCV RNA was examined every 3 months with an Amplicor HCV monitor assay [18]. HCV genotype was examined using antibody serotyping method (HCV serotype 1 and 2 correspond to genotype 1a/1b and 2a/2b, respectively) [19–21]. Histological staging and grading were determined according to the scale Ishak et al. described previously [22]. The control group comprised 16 healthy volunteers with normal serum alanine aminotransferase (ALT) levels and negative test results for serum HCV antibody and hepatitis B surface antigen. Informed consent was obtained from all subjects. This study was approved by the Ethical Review Committee of Jichi Medical School.

2.2. Hepatitis C virus proteins

Recombinant HCV nucleocapsid protein (JCC-2), a gift from the Chemo-Sero-Therapeutic Research Institute (Kumamoto, Japan), was used to study HCV core antigen-specific T-lymphocyte responses. JCC-2 corresponds to HCV of genotype 1b nucleocapsid amino acid residues 1–120.

Recombinant non-structural protein (C7), a gift from the Advanced Life Science Institute (Saitama, Japan), was used to study HCV NS3 antigen-specific responses. C7 corresponds to HCV of genotype 1b non-structural protein amino acid residues 1221–1473.

Although JCC-2 was not a fusion protein, C7 was a fusion protein. Therefore, we purchased synthesized fusion peptide (16 amino acids, Sequence: H-MKAIFVLKGSLDRDPE-OH) from Mimotopes (Clayton Victoria, Australia), and confirm that the peptide does not stimulate PBMCs from both chronic hepatitis C patients and healthy controls in proliferation assay and ELISpot assay.

2.2.1. Isolation of peripheral blood mononuclear cells and stimulation with HCV antigens

PBMCs were isolated from freshly heparinized blood on Ficoll-Paque (Amersham-Pharmacia Biotech, Uppsala, Sweden) gradients and were washed three times in RPMI-1640 medium (GIBCO, Grand Island, NY) with 10% fetal calf serum (FCS). For separating antigen-presenting cells, 1.0×10^7 cells were used. The remaining cells were used for proliferation assays and ELISpot assays. Five sets of PBMCs (each set contained 3.6×10^6 cells) were suspended in 1 ml of RPMI-1640 medium with 10% human AB serum together with either 10 mg/ml of JCC-2, 10 mg/ml of C7, 10 mg/ml of PHA-P, 10 mg/ml of PPD or medium alone (control). PBMCs were then incubated for 4 h at 37 °C in a humid atmosphere with 5% CO_2. After incubation, each set was washed once in RPMI-1640 medium with 10% human AB serum. In each set, 6.0×10^5 cells were used for proliferation assay and 3.0×10^6 cells for ELISpot assay. PHA-P-stimulated PBMCs were used as positive controls in ELISpot assay, and PHA-P-stimulated PBMCs and PPD-stimulated PBMCs were used as positive controls in proliferation assay.

Table 1
Characteristics of patients and healthy controls studied

	Total patients	Patients (liver biopsy)[a]	Controls
n	30	17	16
Age (years)	51.5 (44.0–58.5)	54.0 (49.0–62.0)	33.0 (29.3–49.1)
Gender (M/F)	20/10	13/4	6/10
Serotype (1/2/NTS)	10/19/1	7/10/0	0/0/16
HCV RNA (kcopy/ml)	86.0 (27.3–155.0)	120.0 (61.0–205.0)	ND
ALT (IU/ml)	110.0 (57.8–164.0)	112.0 (53.5–168.5)	<30
PBMC proliferation in response to core antigen	1.234 (0.729–2.138)	1.111 (0.712–1.890)	1.476 (1.042–1.598)
PBMC proliferation in response to NS3 antigen	2.021 (1.136–2.890)	2.200 (0.919–4.198)	1.342 (0.764–1.916)

Values are median and interquartile range. NTS, no type-specific reactivity; ND, not detective; ALT, alanine aminotransferase.
[a] Patients who underwent liver biopsy among 30 total patients.

2.2.2. Proliferation assay for peripheral blood mononuclear cells

HCV antigen-stimulated PBMCs were cultured in 96-well flat-bottomed microculture plates at a density of 2.0×10^5 cells/well with 100 ml of RPMI-1640 medium containing 10% human AB serum in triplicate at 37 °C in a humid atmosphere with 5% CO_2. After 72 h incubation, 10 mM 5-bromodeoxy-2′-deoxyuridine (BrdU) was added to label cells. After 18 h incubation, labeling medium was removed and plates were dried. PBMCs were fixed and DNA was denatured using ethanol. PBMCs were incubated with peroxidase-labeled anti-BrdU. After washing the plate, BrdU incorporated into DNA was measured using an enzyme-linked immunosorbent assay system (Cell Proliferation ELISA system version 2, Amersham-Pharmacia Biotech, Uppsala, Sweden). HCV antigen-specific proliferative response was expressed as stimulation index (SI) calculated from the following formula: SI = (absorbance at 450 nm of HCV antigen-stimulated well − absorbance of medium-alone well)/(absorbance of control well − absorbance of medium-alone well). Proliferative response was considered positive when SI was higher than 2.

2.2.3. ELISpot assay for peripheral blood mononuclear cells

The ELISpot assay was performed using a 96-well microtiter plate with a nitrocellulose membrane bottom (Millititer, Millipore Co., Bedford, MA, USA). The plate was coated with 100 ml of anti-cytokine monoclonal antibody (anti IFN-γ, anti-IL-4, or IL-10; Mabtech AB, Stockholm, Sweden) at a concentration of 15 mg/ml in phosphate-buffered saline (PBS), then incubated overnight at 4 °C. Unbound antibody was removed by washing six times with Hank's balanced saline solution (HBSS). The plate was blocked using 200 ml of RPMI-1640 containing 10% human AB serum. After washing, HCV antigen-stimulated PBMCs were incubated at a density of 5.0×10^5 cells/well in duplicate with 100 ml of RPMI-1640 medium containing 10% human AB serum at 37 °C in a humid atmosphere with 5% CO_2. After incubation, cells were removed by washing the plate 10 times with PBS containing 0.05% Tween 20 (PBS-T) and once with water. Then, 100 ml of biotin-conjugated monoclonal antibody (Mabtech AB, Stockholm, Sweden) was added to each well, and plates were incubated further for 3 h at room temperature. Wells were washed six times with PBS-T and incubated with 100 ml streptavidin–alkaline phosphatase (Mabtech AB, Stockholm, Sweden) for 2 h. Unbound antibodies were removed by washing six times with PBS-T and one time with PBS without Tween 20. Next, 100 ml of alkaline phosphatase substrate (Bio-Rad Laboratories, Richmond, CA, USA) was added to each well and incubated until dark spots emerged. Color development was stopped by washing three times with water, and plates were allowed to dry. Using a dissection microscope, number of spot-forming cells (SFCs) per well was counted. Numbers of HCV antigen-specific SFCs were calculated by subtracting mean number of SFCs from two control wells (without stimulus) from mean number of SFCs from two wells stimulated by HCV antigens.

2.2.4. Isolation of liver infiltrating lymphocytes

Liver tissue (10 mm long) was washed three times with AIM-V (GIBCO, Grand Island, NY, USA) containing 10% human type AB serum and scraped carefully with the point of a needle to separate liver-derived lymphocytes. LILs (about 104–105 mononucleocytes) were isolated from cell suspension by Ficoll-Paque density centrifugation and washed three times with the same medium.

2.2.5. Isolation of antigen presenting cells

The cell suspension containing PBMCs was cultured in polystyrene Petri dishes at 37 °C in a humid atmosphere with 5% CO_2. After 1 h culture, the cell suspension containing non-adherent cells was removed, and the dish was washed three times with HBSS without 2% FCS. Adherent cells were removed using a cell scraper (Becton, Dickinson and Company, Becton Drive, Franklin Lakes, NJ, USA), and suspended in cold HBSS. The cell suspension was washed three times and divided into three 1 ml aliquots for incubation with 10 mg/ml of JCC-2, 10 mg/ml of C7, 10 mg/ml of PHA-P or medium alone for 4 h at 37 °C in a humid atmosphere with 5% CO_2.

2.2.6. ELISpot assay for liver infiltrating lymphocytes

After culture with or without antigens, suspensions of adherent cells were incubated with or without LILs (adherent cells: 50,000 cells/well; LILs: 5000 cells/well) for ELISpot assay for 18 h at 37 °C in a humid atmosphere with 5% CO_2. Since the use of antigen presenting cells in ELISpot assay of LILs increased HCV antigen-specific SFCs, the frequencies of SFCs in antigen presenting cells alone were subtracted in this assay. HCV antigen-specific SFCs were calculated by subtracting number of SFC from control well (without stimulus) from number of SFCs from well stimulated by HCV antigens.

2.3. Statistical analyses

Differences between two groups were compared using the non-parametric Wilcoxon rank sum test. Correlations between two groups were studied using Spearman's correlation coefficient. In multiple statistical comparisons on the same data pool, statistical analyses were made by Bonferoni's method. All statistical analyses were performed using JMP software version 4 for Windows (SAS Institute, Cary, NC, USA).

3. Results

Fig. 1 shows frequencies of HCV antigen-specific cytokine-secreting cells in PBMCs from patients with chronic hepatitis C and healthy controls. Both HCV core and NS3

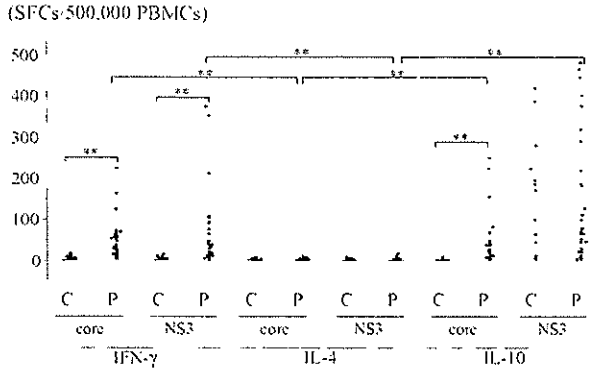

Fig. 1. Frequencies of HCV antigen-specific cytokine-producing cells in PBMCs in patients and controls. Box plots summarize distributions of points at each factor level. Boxes end at the 25th and 75th quantiles. The median is also expressed within the box. C, controls; P, patients; $^{**}p < 0.01$.

antigens stimulated IFN-γ production by PBMCs from patients with chronic hepatitis C but not by PBMCs from healthy controls. HCV core antigen also stimulated specifically IL-10 production by PBMCs from patients with chronic hepatitis C. However, HCV NS3 antigen stimulated IL-10 production by PBMCs from both patients with chronic hepatitis C and healthy controls, indicating that HCV NS3 antigen could stimulate non-specifically IL-10 production by PBMCs. Both HCV core antigen-specific and NS3 antigen-specific IL-4-secreting cells were hardly detectable in PBMCs from both patients with chronic hepatitis C and healthy controls, although PHA-P stimulated IL-4-secreting cells were abundantly detected (data not shown).

Fig. 2 shows the frequencies of HCV antigen-specific cytokine-secreting cells in LILs in patients with chronic hepatitis C. Both HCV core antigen- and NS3 antigen-specific IL-4-secreting cells were hardly detectable in LILs from patients with chronic hepatitis C, although PHA-P stimulated IL-4-secreting LILs were abundantly detected (data not shown).

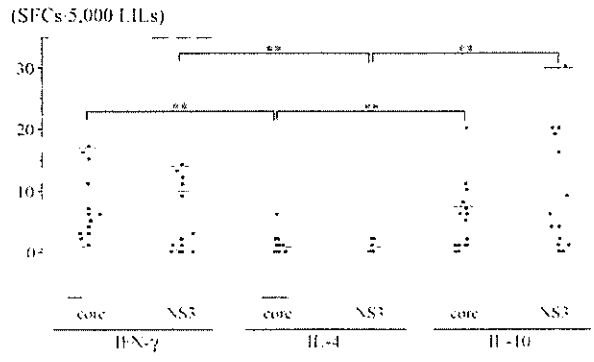

Fig. 2. Frequencies of HCV antigen-specific cytokine-producing cells in LILs in patients. Box plots summarize distributions of points at each factor level. Boxes end at the 25th and 75th quantiles. The median is also expressed within the box. C, controls; P, patients; $^{**}p < 0.01$.

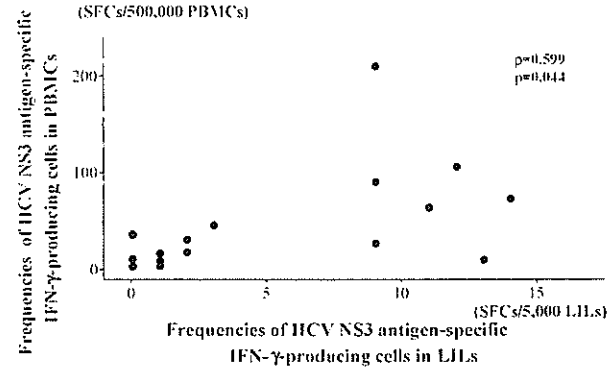

Fig. 3. Correlation coefficient between frequencies of HCV NS3 antigen-specific IFN-γ-producing cells in PBMCs and LILs. ρ, Spearman's correlation coefficient.

Frequencies of HCV NS3 antigen-specific IFN-γ-secreting cells in PBMCs correlated significantly with those in LILs as shown in Fig. 3. Frequencies of HCV NS3 antigen-specific IL-10-secreting cells in PBMCs also correlated significantly with those in LILs as shown in Fig. 4. On the other hand, the correlation between frequencies of HCV core antigen-specific IFN-γ-secreting cells in PBMCs and those in LILs and the correlation between frequencies of HCV core antigen-specific IL-10-secrreting cells in PBMCs and those in LILs did not reach statistical significance. Although frequencies of HCV core antigen-specific and NS3 antigen-specific IFN-γ-secreting cells in LILs did not correlate with these of HCV core antigen-specific and NS3 antigen-specific IL-10-secreting cells in LILs, frequencies of HCV core antigen-specific IFN-γ-secreting cells in PBMCs correlated significantly with both those of HCV core antigen-specific IL-10-secreting cells in PBMCs (Fig. 5) and those of HCV NS3 antigen-specific IL-10-secreting cells in PBMCs (Fig. 6).

HCV antigen-specific proliferative responses of PBMCs in 30 patients with chronic hepatitis C and 16 healthy controls are shown in Table 1. PHA-P and PPD stimulated prolifera-

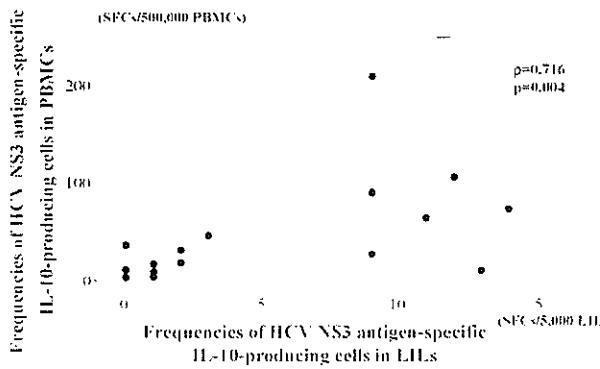

Fig. 4. Correlation coefficient between frequencies of HCV NS3 antigen-specific IL-10-producing cells in PBMCs and LILs. ρ, Spearman's correlation coefficient.

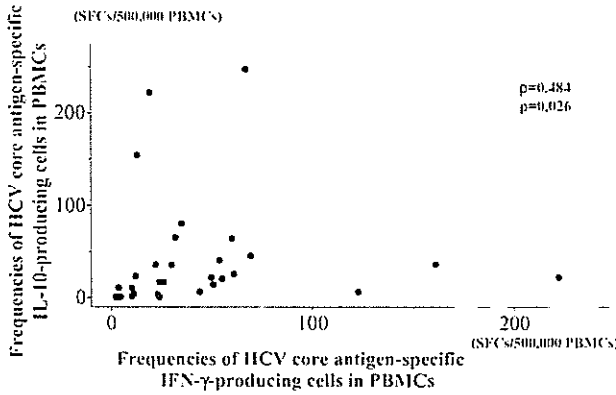

Fig. 5. Correlation coefficient between frequencies of HCV core antigen-specific IFN-γ-producing cells and frequencies of HCV core antigen-specific IL-10-producing cells in PBMCs. ρ, Spearman's correlation coefficient.

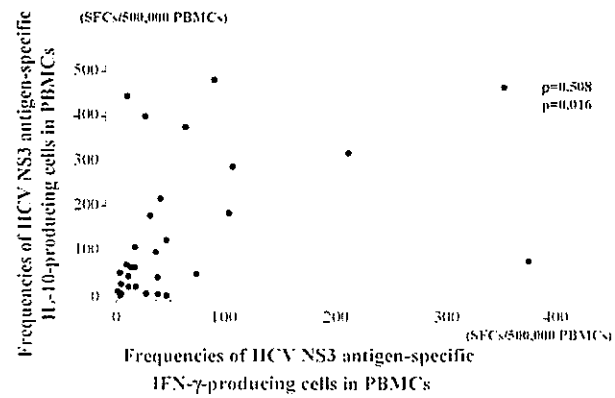

Fig. 6. Correlation coefficient between frequencies of HCV NS3 antigen-specific IFN-γ-producing cells and frequencies of HCV NS3 antigen-specific IL-10-producing cells in PBMCs. ρ, Spearman's correlation coefficient.

tive response were positive in all patients and controls (data not shown). Proliferative responses were positive in 9 of the 30 patients (30.0%) and 2 of the 16 healthy controls (13.0%) for HCV core antigen stimulation, and in 15 patients (50.0%) and 3 healthy controls (19.0%) for HCV NS3 antigen stimulation.

There were no significant correlations between serum ALT levels, HCV RNA levels, serotype, histological grades, HCV core and NS3 antigen-specific proliferative response and number of HCV antigen-specific IFN-γ- or IL-10-secreting cells (data not shown).

4. Discussion

Our study shows that the immune response to HCV antigens was correlated between LILs and PBMCs even though HCV antigen-specific T cells are far more abundant in liver tissue than in peripheral blood. These finding seems to suggest that we could confirm the adequacy of using PBMCs to study the host immune response to HCV-specific antigens in substitution for LILs. However, the percentage of HCV antigen-specific cytokine-secreting cells is less than 0.5%, even in LILs. In chronic hepatitis C virus infection, non-specific T cells and/or the other kinds of immune cells may play more crucial roles at sites of inflammation as inflammation increases in severity. Hultgren et al. reported that the presence of an NS3-specific T-cell response was related to the viral genotype; a T cell response was more common among those infected by genotype 3, as compared to those infected with genotype 1 [23]. However, in this study, the immune response of patients with chronic HCV infection (genotype were 1a/1b and 2a/2b) to HCV antigens seemed identical. Therefore there were no apparent correlation between frequencies of HCV antigen-specific cytokine-secreting cells and serotype, viral load, ALT levels and histological grades as observed in patients with chronic hepatitis B [24].

In both LILs and PBMCs, HCV antigens-specific IL-4-secreting cells were hardly detectable, although HCV antigen-specific IFN-γ-secreting cells were easily detectable. This result is similar to our recent finding in patients with chronic hepatitis B [24]. The finding indicate that helper T-cell responses to HCV antigens are shifted to Th1. In acute self-limited HCV infection, the vigorous immune responses to HCV NS3 antigen that produces Th1-derived IFN-γ may play a decisive role in viral clearance [13], and in chronic hepatitis C virus infection, insufficient systemic type 1 cytokine secretion by PBMCs might be associated with increased viral load and disease progression [12].

HCV antigens-specific IL-10-secreting cells were detectable in both LILs and PBMCs from patients with chronic HCV infection and even in PBMCs from healthy controls, and the frequencies were comparable to those of HCV antigens-specific IFN-γ-secreting cells. Moreover, some healthy controls were positive for HCV antigen-specific proliferative responses. This may be due to the fact that healthy controls were hospital workers who might have been exposed to HCV previously as reported by Koziel et al. [25]. Although there is a possibility of cross-reaction between HCV NS3 antigen and other natural antigens caused by molecular mimicry, the fact that the high percentage of controls and patients were positive for HCV NS3 antigen-stimulated IL-10 production suggest that HCV NS3 may stimulate non-specifically IL-10 production by PBMCs as HCV NS4 has been proven to do so [26]. MacDonald et al. reported that HCV core antigen-specific $CD4^+$ Tr1 cells might contribute to disease chronicity and $CD4^+$ Th1 and Tr cells were induced against the same epitopes on the core protein in HCV [27], and Cabrera et al. assessed and reported the immunomodulatory role of the IL-10-secreting cells ($CD4^+CD25^+$ regulatory T lymphocytes) in HCV infection [28]. Wertheimer et al. investigated T cell determinants within NS3 antigen in subjects with HCV infection using IFN-γ-production with an ELISpot assay [29]. However, whether the NS3 epitopes

recognized by IFN-γ- and IL-10-secreting cells are the same is unknown. Thus, if distinct epitopes are recognized, identifying the epitopes that do not stimulate IL-10-secreting cells but do stimulate IFN-γ-secreting cells may contribute to the development of a cell-mediated anti-HCV vaccine.

Acknowledgements

This study was supported in past grant from the Ministry of Education, Culture, Sports, Science and Technology of Japan and the Ministry of Health, Labor and Welfare of Japan.

References

[1] Lauer GM, Walker BD. Hepatitis C virus infection. New Engl J Med 2001;345(1):41–52.
[2] Tsai SL, Liaw YF, Chen MH, et al. Detection of type 2-like T-helper cells in hepatitis C virus infection: implications for hepatitis C virus chronicity. Hepatology 1997;25(2):449–58.
[3] Iwata K, Wakita T, Okumura A, et al. Interferon gamma production by peripheral blood lymphocytes to hepatitis C virus core protein in chronic hepatitis C infection. Hepatology 1995;22(4 Pt. 1):1057–64.
[4] Chang KM, Thimme R, Melpolder JJ, et al. Differential CD4(+) and CD8(+) T-cell responsiveness in hepatitis C virus infection. Hepatology 2001;33(1):267–76.
[5] Mori H, Yabu K, Yoshizawa K, et al. Lymphocyte proliferative responses to recombinant hepatitis C virus antigens in patients with chronic hepatitis C. J Gastroenterol Hepatol 1996;11(8):697–704.
[6] Missale G, Bertoni R, Lamonaca V, et al. Different clinical behaviors of acute hepatitis C virus infection are associated with different vigor of the anti-viral cell-mediated immune response. J Clin Invest 1996;98(3):706–14.
[7] Diepolder HM, Zachoval R, Hoffmann RM, et al. Possible mechanism involving T-lymphocyte response to non-structural protein 3 in viral clearance in acute hepatitis C virus infection. Lancet 1995;346(8981):1006–7.
[8] Yang PM, Hwang LH, Lai MY, et al. Prominent proliferative response of peripheral blood mononuclear cells to a recombinant non-structural (NS3) protein of hepatitis C virus in patients with chronic hepatitis C. Clin Exp Immunol 1995;101(2):272–7.
[9] Ferrari C, Valli A, Galati L, et al. T-cell response to structural and non-structural hepatitis C virus antigens in persistent and self-limited hepatitis C virus infections. Hepatology 1994;19(2):286–95.
[10] Botarelli P, Brunetto MR, Minutello MA, et al. T-lymphocyte response to hepatitis C virus in different clinical courses of infection. Gastroenterology 1993;104(2):580–7.
[11] Schupper H, Hayashi P, Scheffel J, et al. Peripheral-blood mononuclear cell responses to recombinant hepatitis C virus antigens in patients with chronic hepatitis C. Hepatology 1993;18(5):1055–60.
[12] Lechmann M, Woitas RP, Langhans B, et al. Decreased frequency of HCV core-specific peripheral blood mononuclear cells with type 1 cytokine secretion in chronic hepatitis C. J Hepatol 1999; 31(6):971–8.
[13] Gerlach JT, Diepolder HM, Jung MC, et al. Recurrence of hepatitis C virus after loss of virus-specific CD4(+) T-cell response in acute hepatitis C. Gastroenterology 1999;117(4):933–41.
[14] Schirren CA, Jung MC, Gerlach JT, et al. Liver-derived hepatitis C virus (HCV)-specific CD4(+) T cells recognize multiple HCV epitopes and produce interferon gamma. Hepatology 2000;32(3): 597–603.
[15] Lohr HF, Schlaak JF, Kollmannsperger S, et al. Liver-infiltrating and circulating CD4+ T cells in chronic hepatitis C: immunodominant epitopes HLA-restriction and functional significance. Liver 1996;16(3):174–82.
[16] Minutello MA, Pileri P, Unutmaz D, et al. Compartmentalization of T lymphocytes to the site of disease: intrahepatic CD4+ T cells specific for the protein NS4 of hepatitis C virus in patients with chronic hepatitis C. J Exp Med 1993;178(1):17–25.
[17] He XS, Rehermann B, Lopez-Labrador FX, et al. Quantitative analysis of hepatitis C virus-specific CD8(+) T cells in peripheral blood and liver using peptide-MHC tetramers. Proc Natl Acad Sci USA 1999;96(10):5692–7.
[18] Young KK, Resnick RM, Myers TW. Detection of hepatitis C virus RNA by a combined reverse transcription-polymerase chain reaction assay. J Clin Microbiol 1993;31(4):882–6.
[19] Tanaka T, Tsukiyama-Kohara K, Yamaguchi K, et al. Significance of specific antibody assay for genotyping of hepatitis C virus. Hepatology 1994;19(6):1347–53.
[20] Tsukiyama-Kohara K, Yamaguchi K, Maki N, et al. Antigenicities of Group I and II hepatitis C virus polypeptides—molecular basis of diagnosis. Virology 1993;192(2):430–7.
[21] Simmonds P, McOmish F, Yap PL, et al. Sequence variability in the 5′ non-coding region of hepatitis C virus: identification of a new virus type and restrictions on sequence diversity. J Gen Virol 1993;74(Pt 4):661–8.
[22] Ishak K, Baptista A, Bianchi L, et al. Histological grading and staging of chronic hepatitis. J Hepatol 1995;22(6):696–9.
[23] Hultgren C, Desombere I, Leroux-Roels G, et al. Evidence for a relation between the viral load and genotype and hepatitis C virus-specific T cell responses. J Hepatol 2004;40(6):971–8.
[24] Hyodo N, Tajimi M, Ugajin T, et al. Frequencies of interferon-γ and interleukin-10-secreting cells in peripheral blood mononuclear cells and liver infiltrating lymphocytes in chronic hepatitis B virus infection. Hepatol Res 2003;27(2):109–16.
[25] Koziel MJ, Wong DK, Dudley D, et al. Hepatitis C virus-specific cytolytic T lymphocyte and T helper cell responses in seronegative persons. J Infect Dis 1997;176(4):859–66.
[26] Brady MT, MacDonald AJ, Rowan AG, et al. Hepatitis C virus non-structural protein 4 suppresses Th1 responses by stimulating IL-10 production from monocytes. Eur J Immunol 2003;33(12):3448–57.
[27] MacDonald AJ, Duffy M, Brady MT, et al. CD4 T helper type 1 and regulatory T cells induced against the same epitopes on the core protein in hepatitis C virus-infected persons. J Infect Dis 2002;185(6):720–7.
[28] Cabrera R, Tu Z, Xu Y, et al. An immunomodulatory role for CD4(+)CD25(+) regulatory T lymphocytes in hepatitis C virus infection. Hepatology 2004;40(5):1062–71.
[29] Wertheimer AM, Miner C, Lewinsohn DM, et al. Novel CD4+ and CD8+ T-cell determinants within the NS3 protein in subjects with spontaneously resolved HCV infection. Hepatology 2003;37(3): 577–89.